A one dimensional model of Earth structure in the western United States from GPS observation of ocean tidal load

Takeo Ito @ caltech and Nagoya Univ,
Mark Simons @ caltech

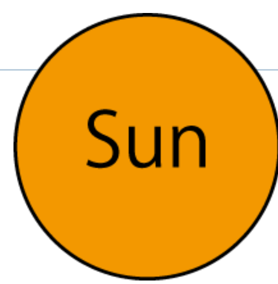

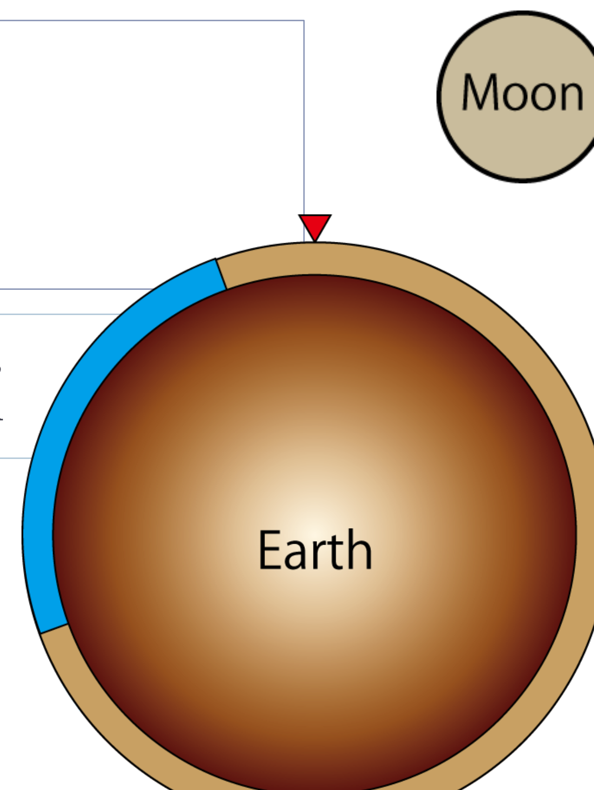

Contents

- Introduction
- Earth tide
  (body tide and OTL [Ocean Tidal Load])
- Earth tide observation using GPS in Japan
- OTL response using GPS in the western United States
- Method
- Results

Introduction

- The Earth tidal data are limited such as gravity, strain meters etc.
- These instruments are very expensive, and observation coverage is sparse.
- GPS provides relatively good coverage.

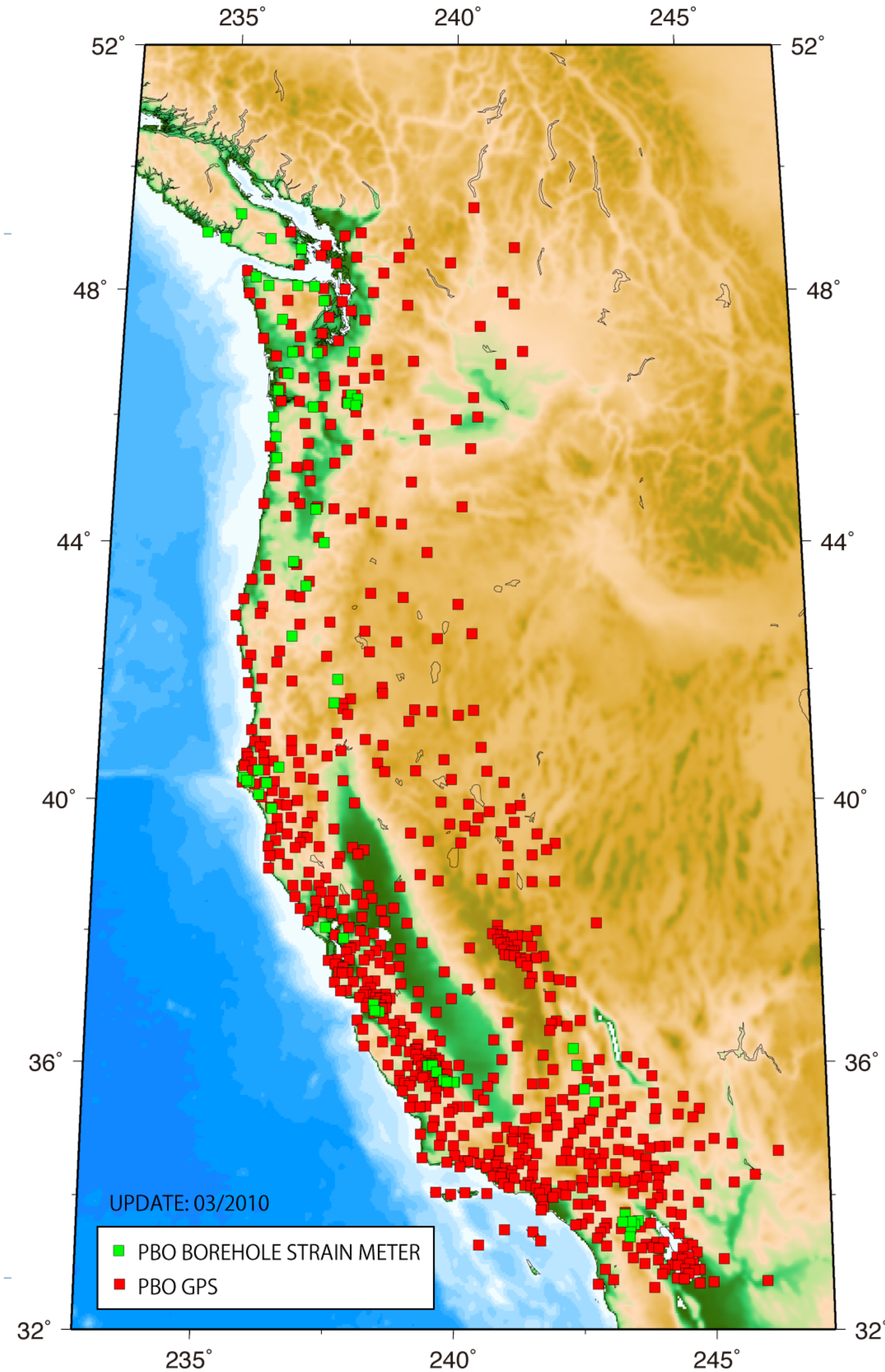

Earth tide

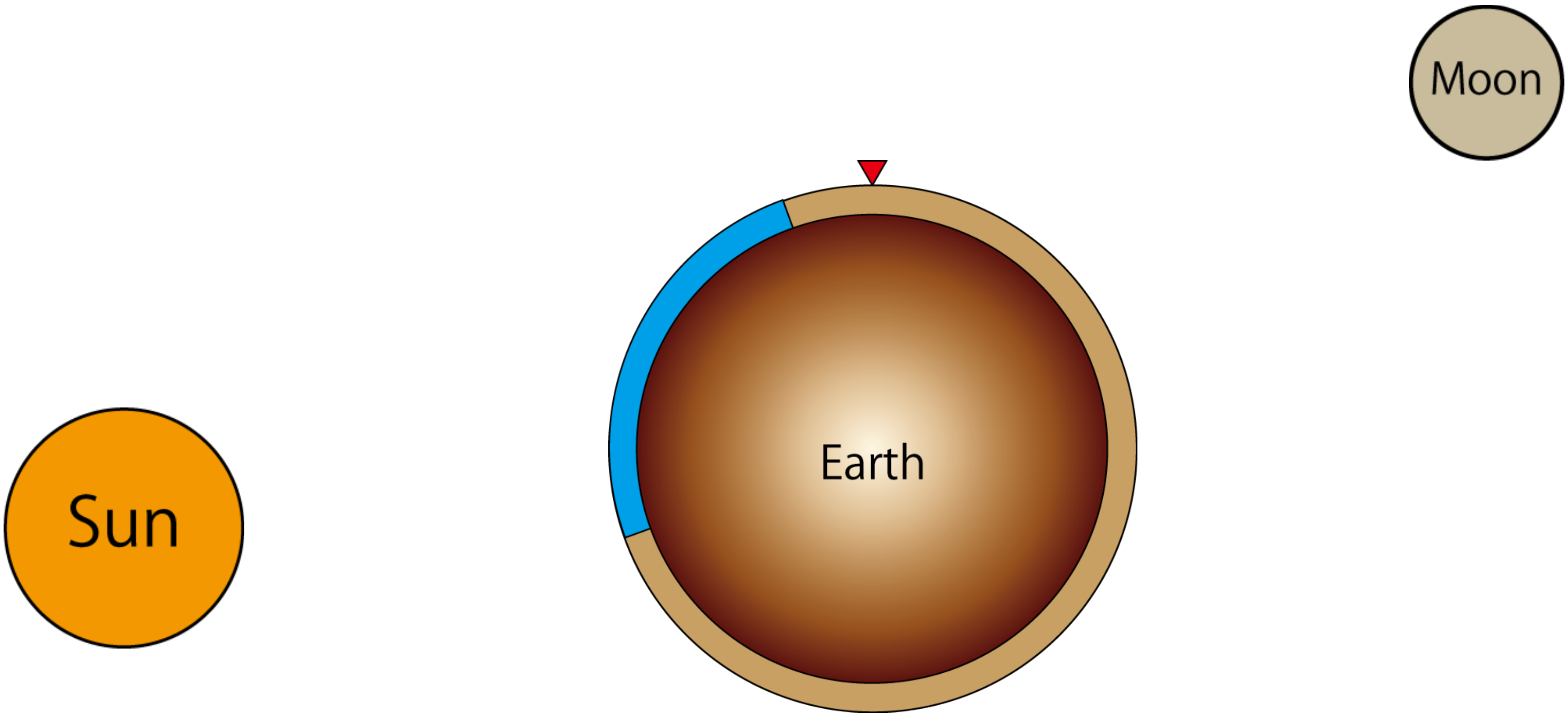

Tidal forcing

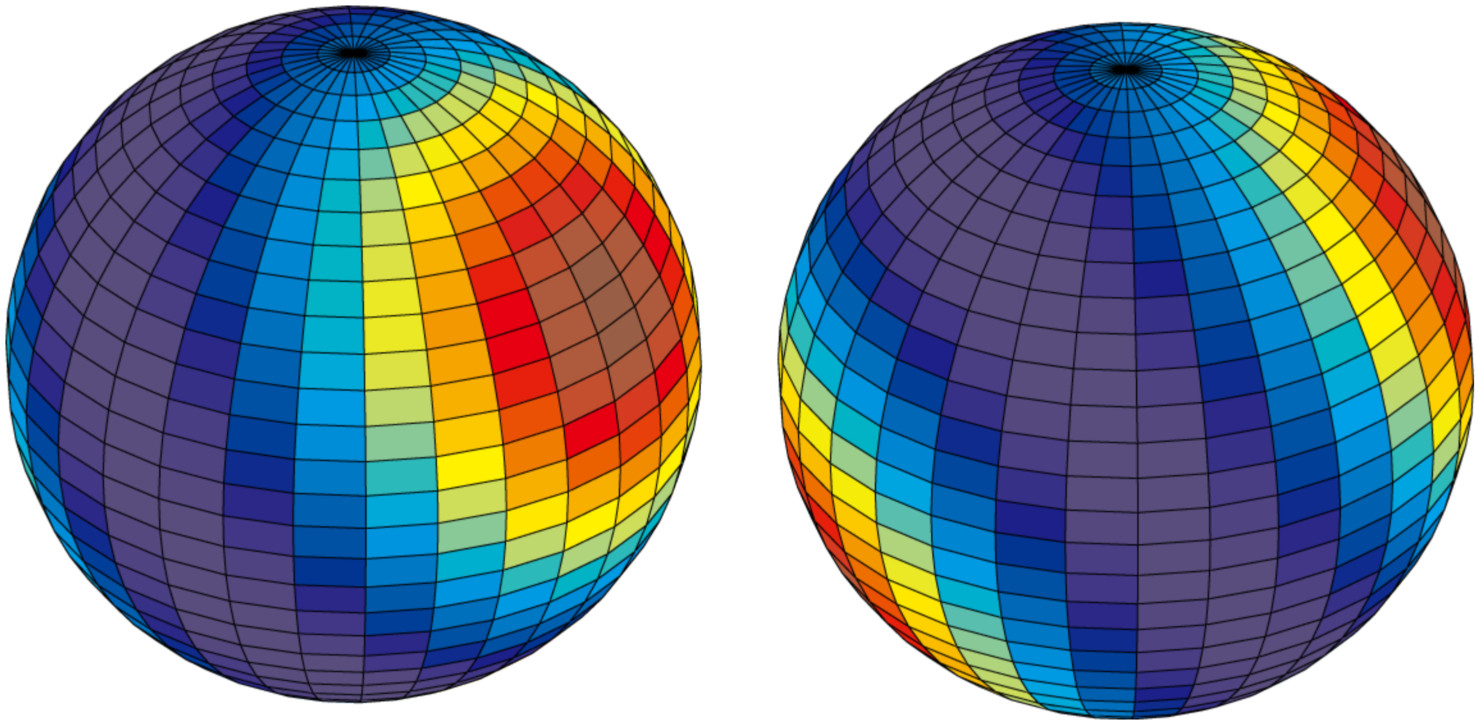

Body tide

- Wavelength is about 40,000km.
  (depend 2 or 3 degrees)

  → same sensitivity of subsurface structure for any tidal constituents.
  → no sensitivity for local variation.

- High accuracy prediction.
  (about 3 micron depend on Earth model)

  → well predictable body tide

- Well known the period of each tidal constitutes.
  (Better than 0.01 sec)

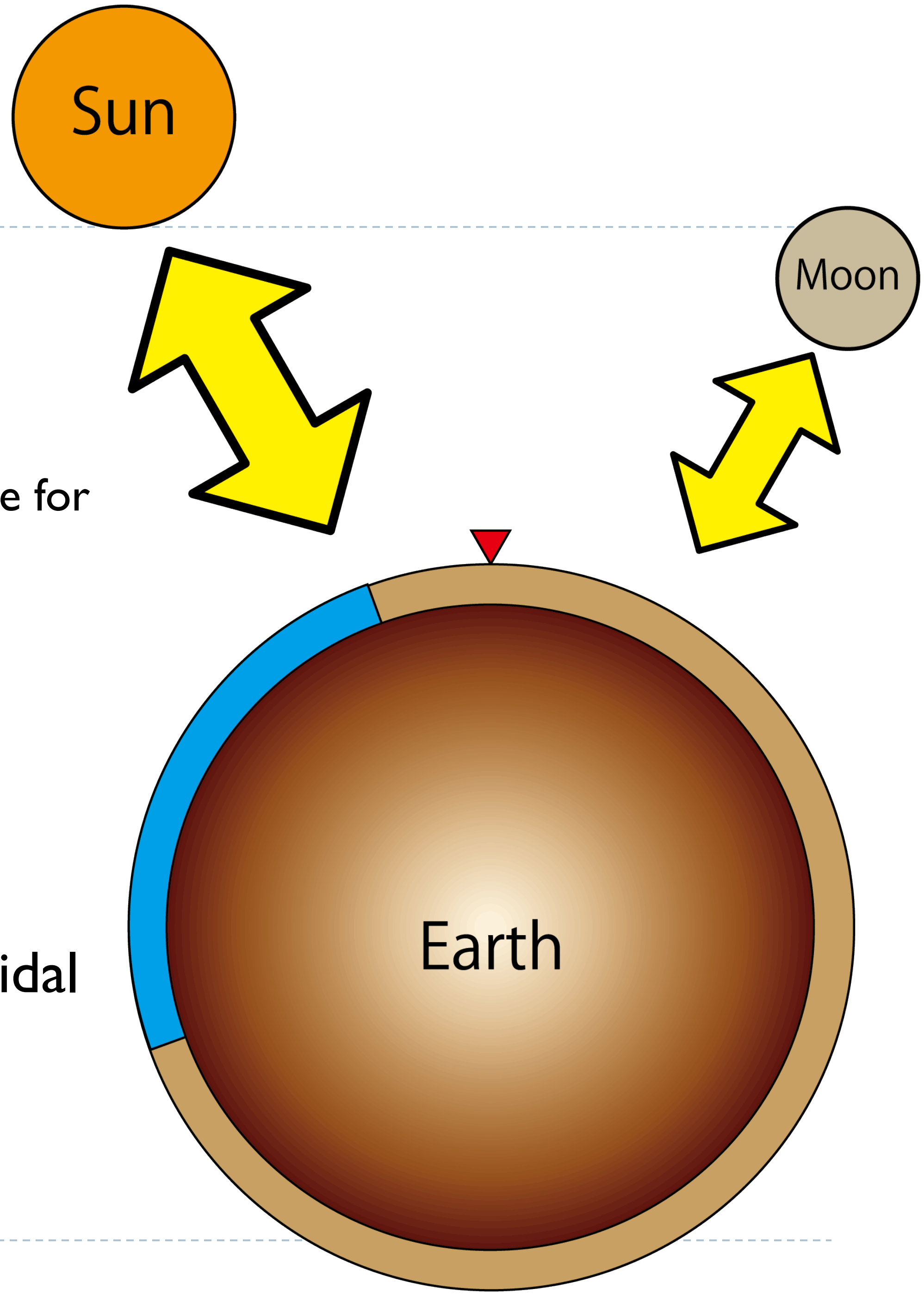

The cycle of tidal deformation

Tidal constitutes	Cycle (hours)	description
M2	12.42060	Principal lunar, semidiurnal
K1	23.93447	Sun-Moon angle, diurnal
S2	12.00000	Principal solar, semidiurnal
O1	25.81934	Principal lunar declinational
P1	24.06589	Principal solar declinational
N2	12.65835	Principal lunar elliptic, semidiurnal
K2	11.96723	Sun-Moon angle, semidiurnal
MF	327.85899	
Q1	26.86836	
MM	661.30919	Lunar evectional constituent
2N2	12.90537	
MTM	219.19039	
S1	24.00000	Principal solar, diurnal
M4	6.21030	Principal lunar, quatdiurnal
MSQM	170.29902	

Ocean tide

- Period of each constituent are well known (same as body tides).
- Ocean tide can be predicted using global ocean tide models.

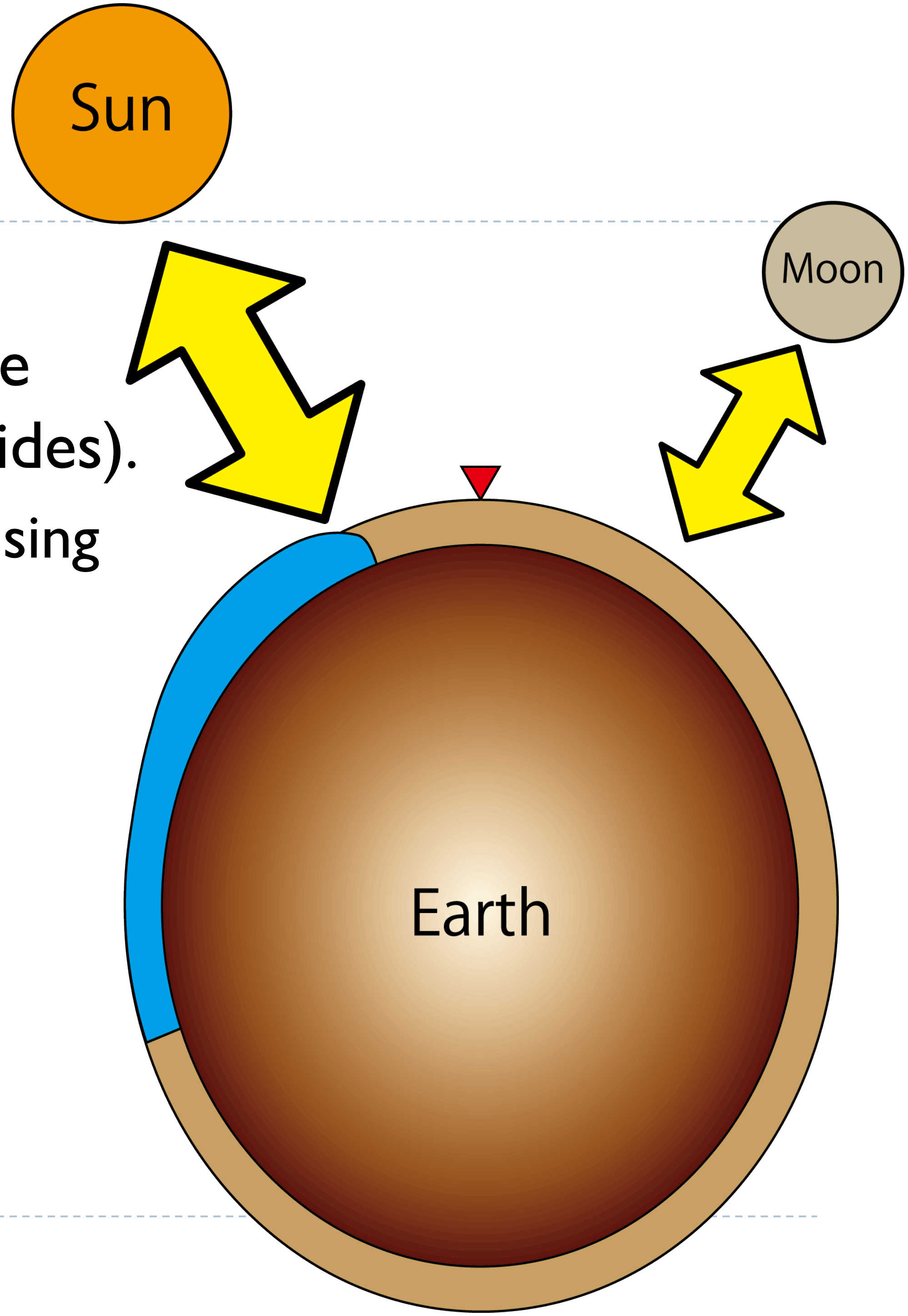

The global ocean tides model

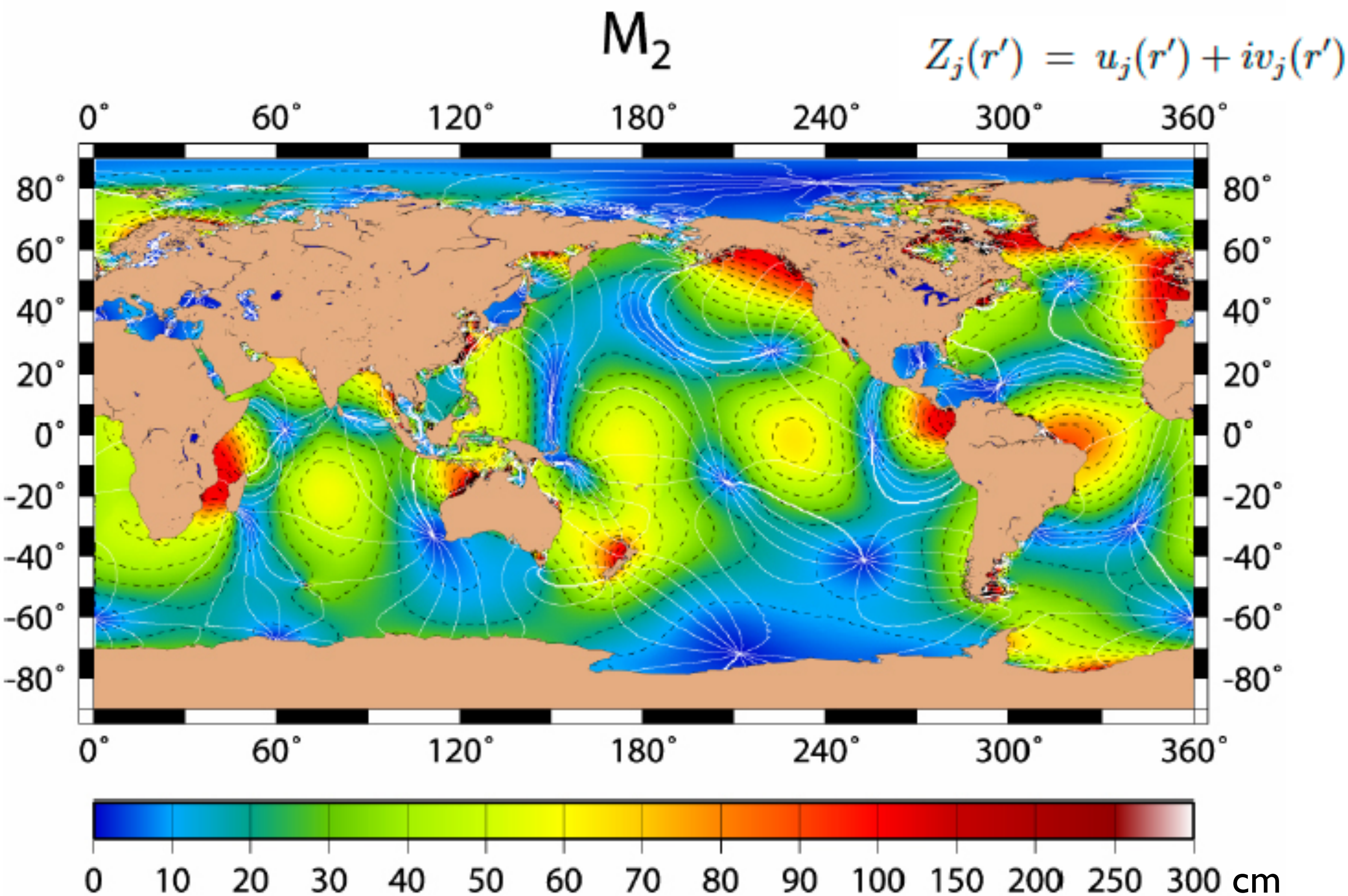

NAO.99b

Ocean Tidal Loading (OTL)

$$L_j(r) = \int_{\Omega} \rho_{sea} G_j(|r - r'|) Z_j(r') d\Omega$$

$L_j(r)$: OTL response of *j*th constituent at *r*

ρ_{sea} : density of sea water (1,035 kg/m3)

$G_j(|r - r'|)$: load Green's function of *j*th constituent

$Z_j(r')$: the tidal height variations at *r*' (complex number)

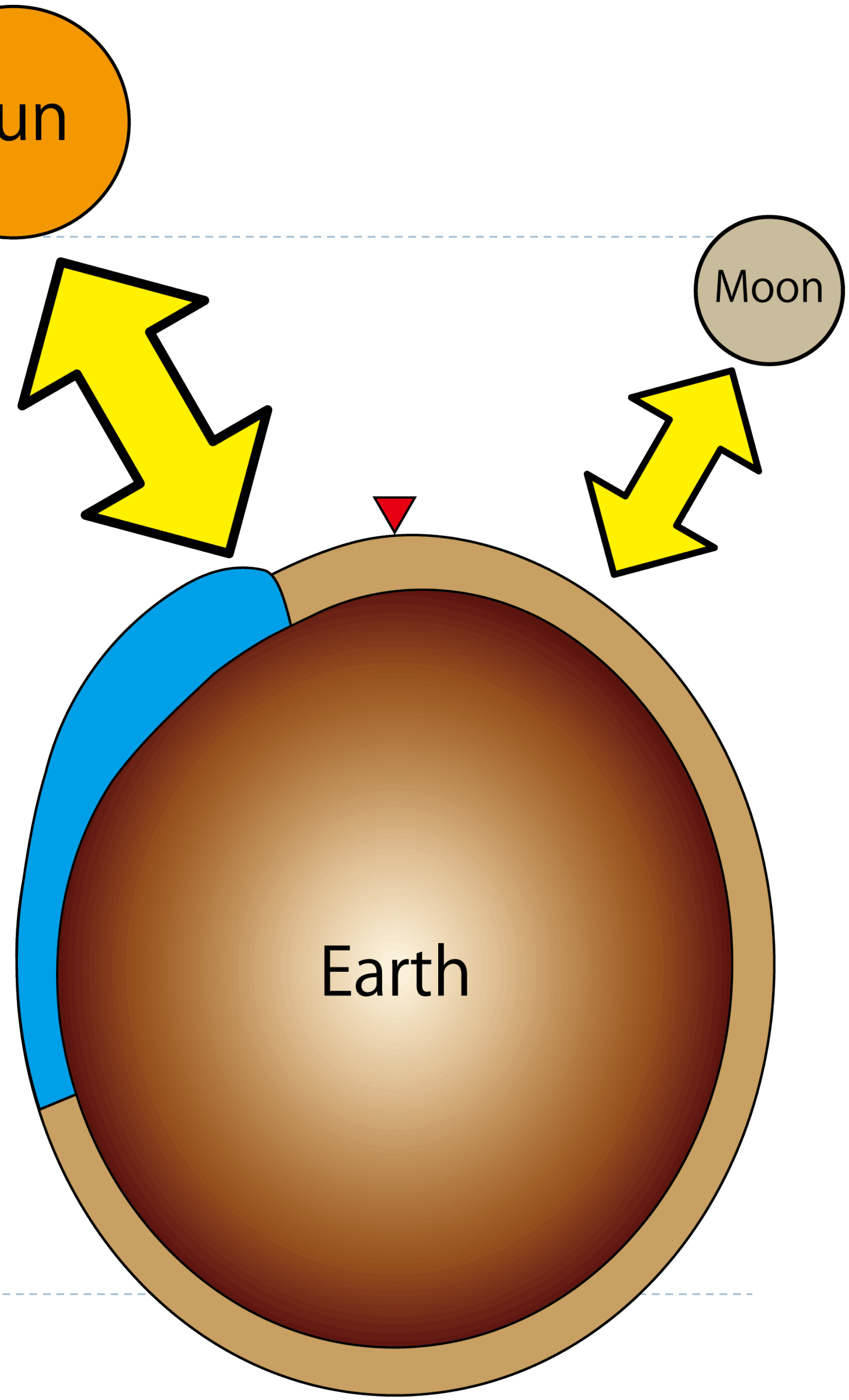

Japan

- GPS: 1200 sites
- Observation periods: 4/1/2006-7/31/2006
- Sampling rate: 30 sec
- GPS software: Gps Tools [ver. 0.6.3] developed by Takasu and Kasai [2005]
- Secular velocity ➔

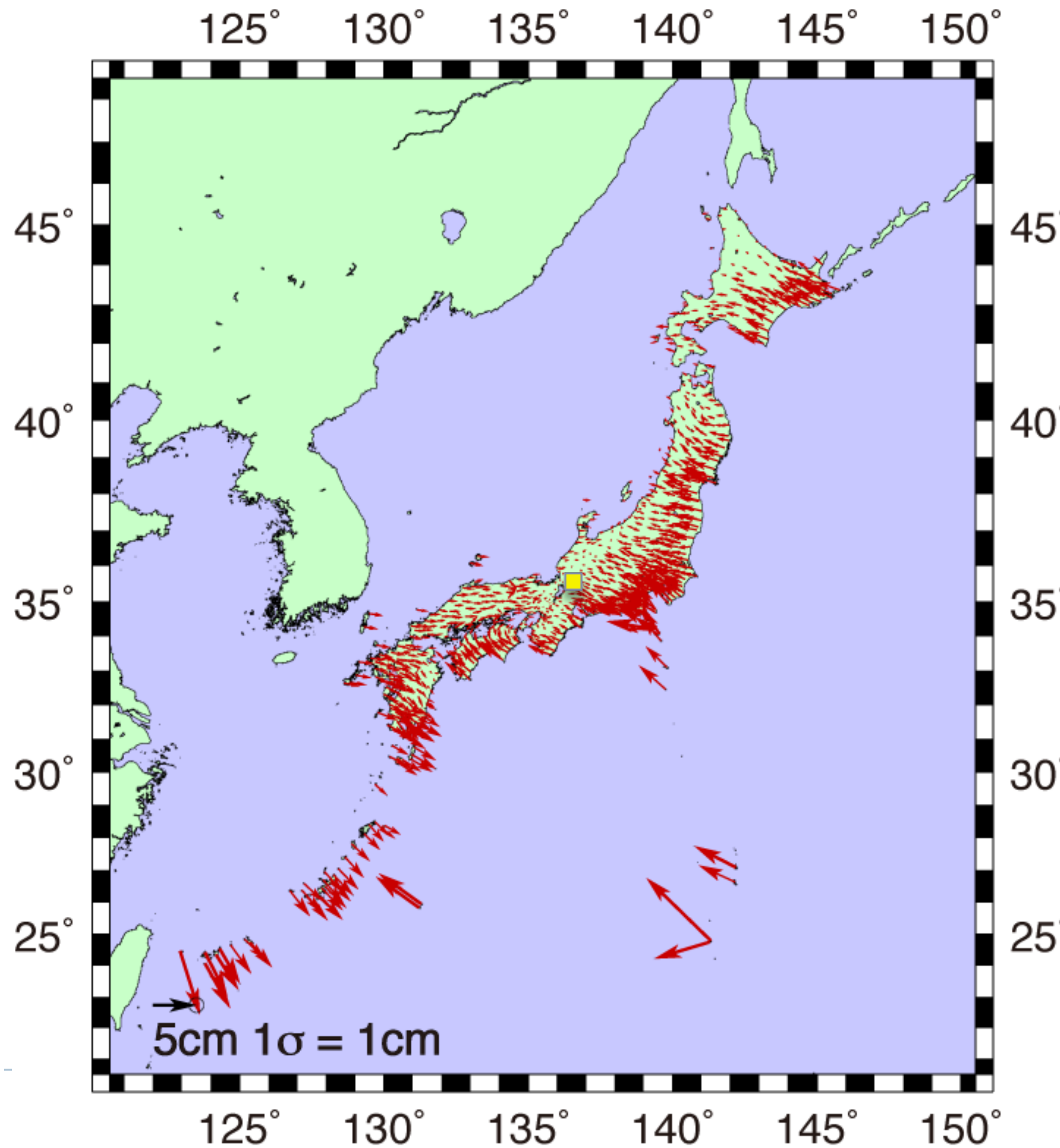

Earth tide observation using GPS (1/3)

- KPPP GPS
  (30 sec sampling)
- Tajimi site
  (center of Japan)
- Period May, 2006.

- Green: Predicted
  (Body tide +OTL)
- Red: GPS

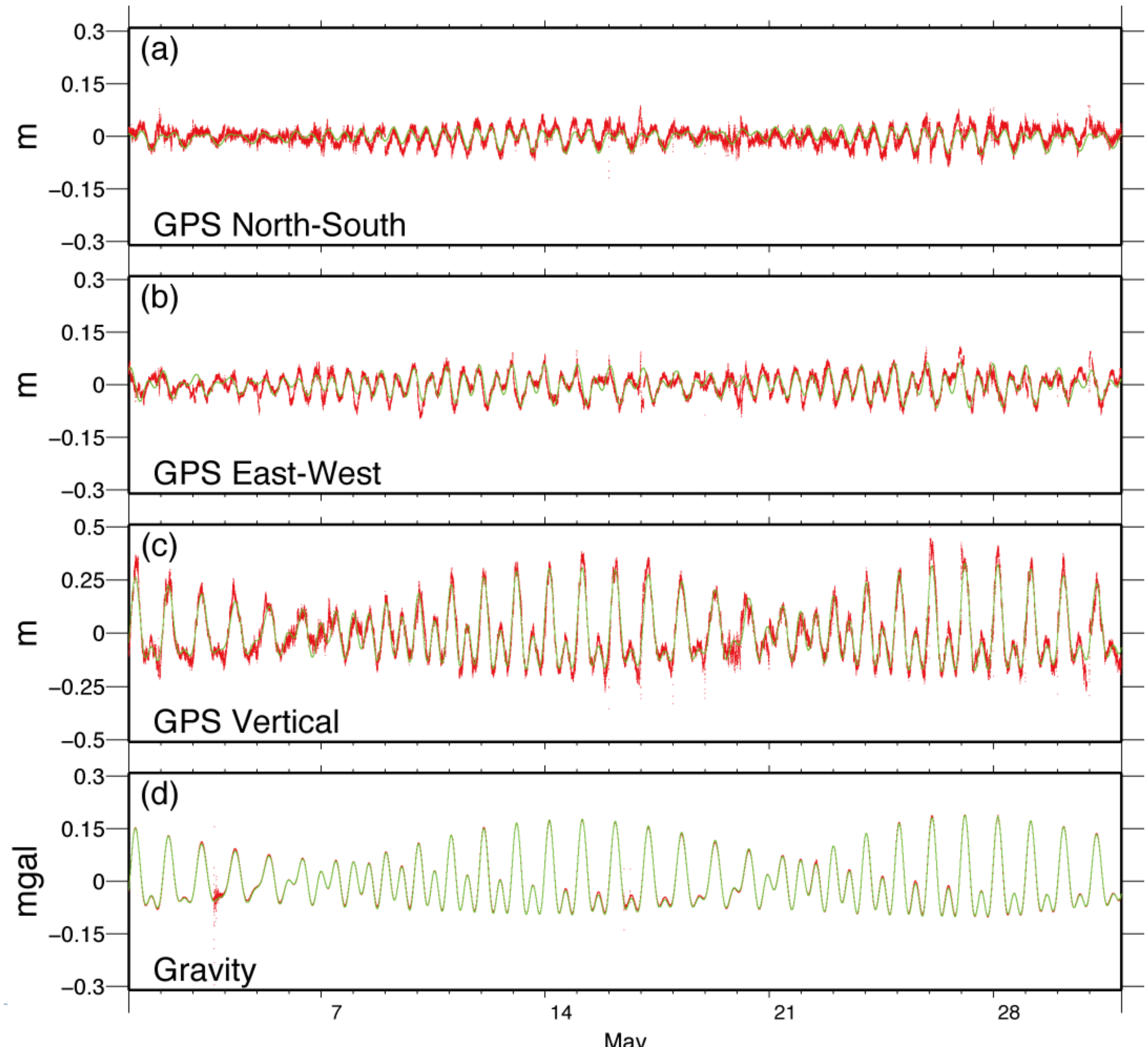

After Ito et al. (2009)

Earth tide observation using GPS (2/3)

- Spectral Analysis

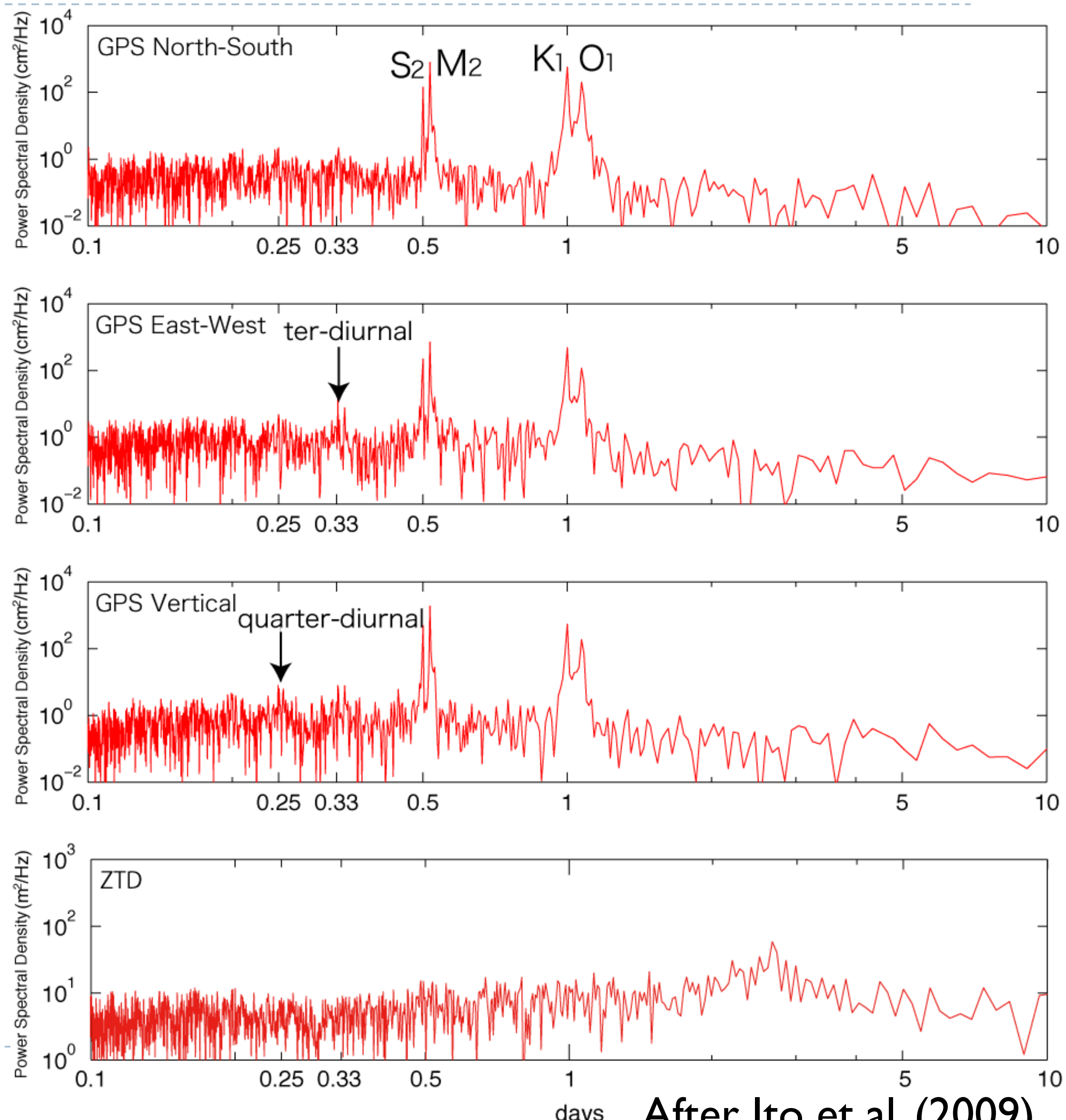

After Ito et al. (2009)

Earth tide observation using GPS (3/3)

- Total tidal signal (body + ocean)
- Hourly snapshots

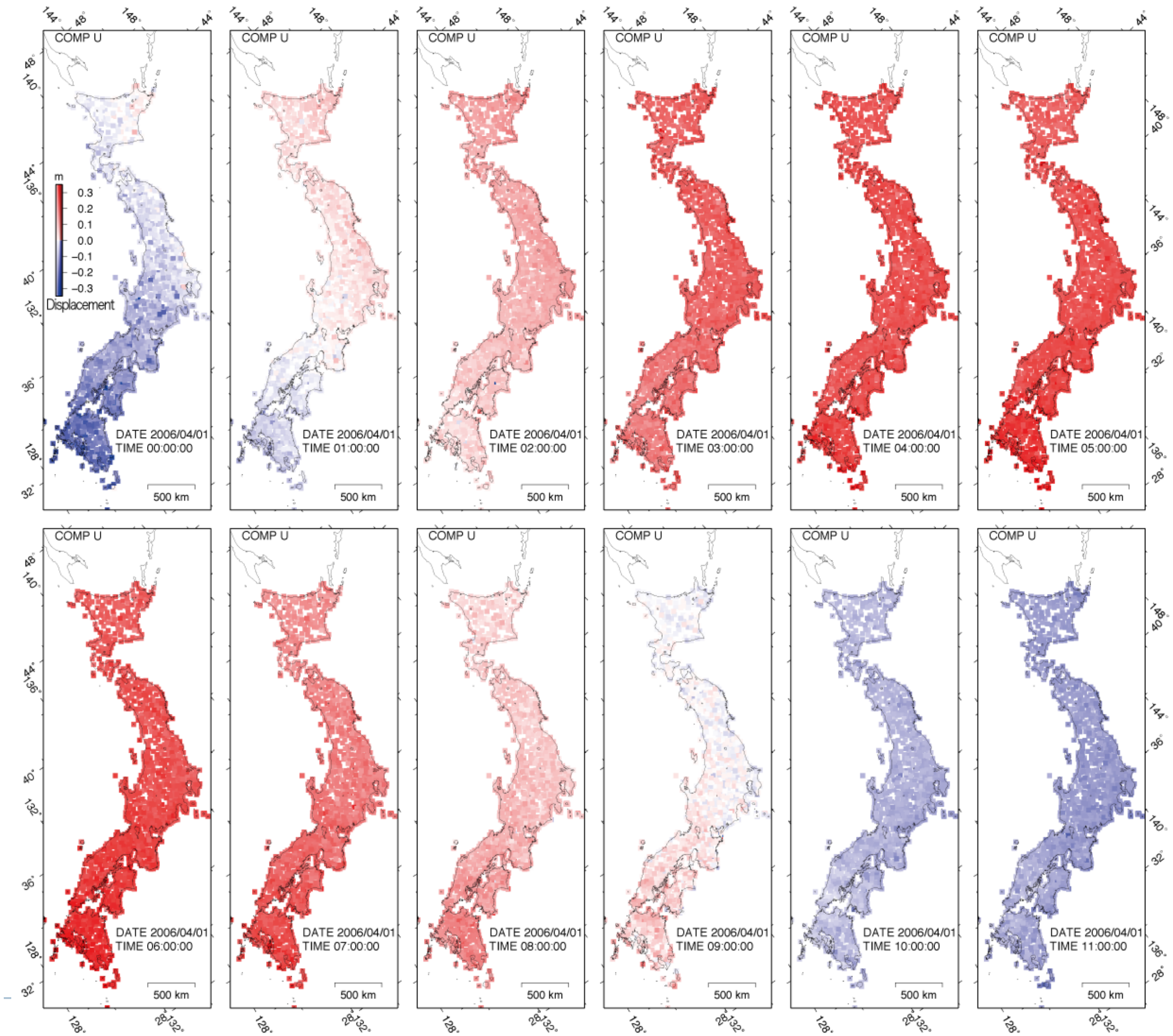

After Ito et al. (2009)

Compare GPS with super-conducting gravimeter

- S2: a cycle of daily orbit discontinuities
- K1: the orbital repeat period of the GPS satellite

Table 1
Summary of tidal coefficients at Tajimi GPS station and super-conducting gravimetry at Inuyama. Each second row indicates the estimated error.

Comp.	Coef.	Lag	Std.	M2		S2		K1		O1	
				Amp.	Phase	Amp.	Phase	Amp.	Phase	Amp.	Phase
N-S	0.61	146	2.13	1.068	1.44	1.534	−2.91	0.928	−27.05	0.939	1.22
				0.0006	0.023	0.0033	0.070	0.0014	0.056	0.0002	0.012
E-W	0.76	971	2.09	0.984	0.26	0.737	−32.45	0.996	−28.73	1.151	0.47
				0.0006	0.026	0.0003	0.001	0.0010	0.049	0.0023	0.075
Vertical	0.94	−363	4.17	1.010	0.19	1.195	−0.91	1.025	3.86	0.977	0.78
				0.0001	0.005	0.0005	0.015	0.0492	0.009	0.0001	0.001
Grav.	0.99	4	1.00	1.009	0.10	1.013	0.31	0.976	−0.196	0.995	0.04
				0.0002	0.002	0.0007	0.005	0.0032	0.003	0.0001	0.001

After Ito et al. (2009)

The spatial perturbation of the Earth tidal field

- Variation relate to sub-surface structure
- The average phase lag is 0.11 degrees of angle.
- The average amplitude ratio is 1.007
- Average structure is fine, but regionally coherent variations are apparent

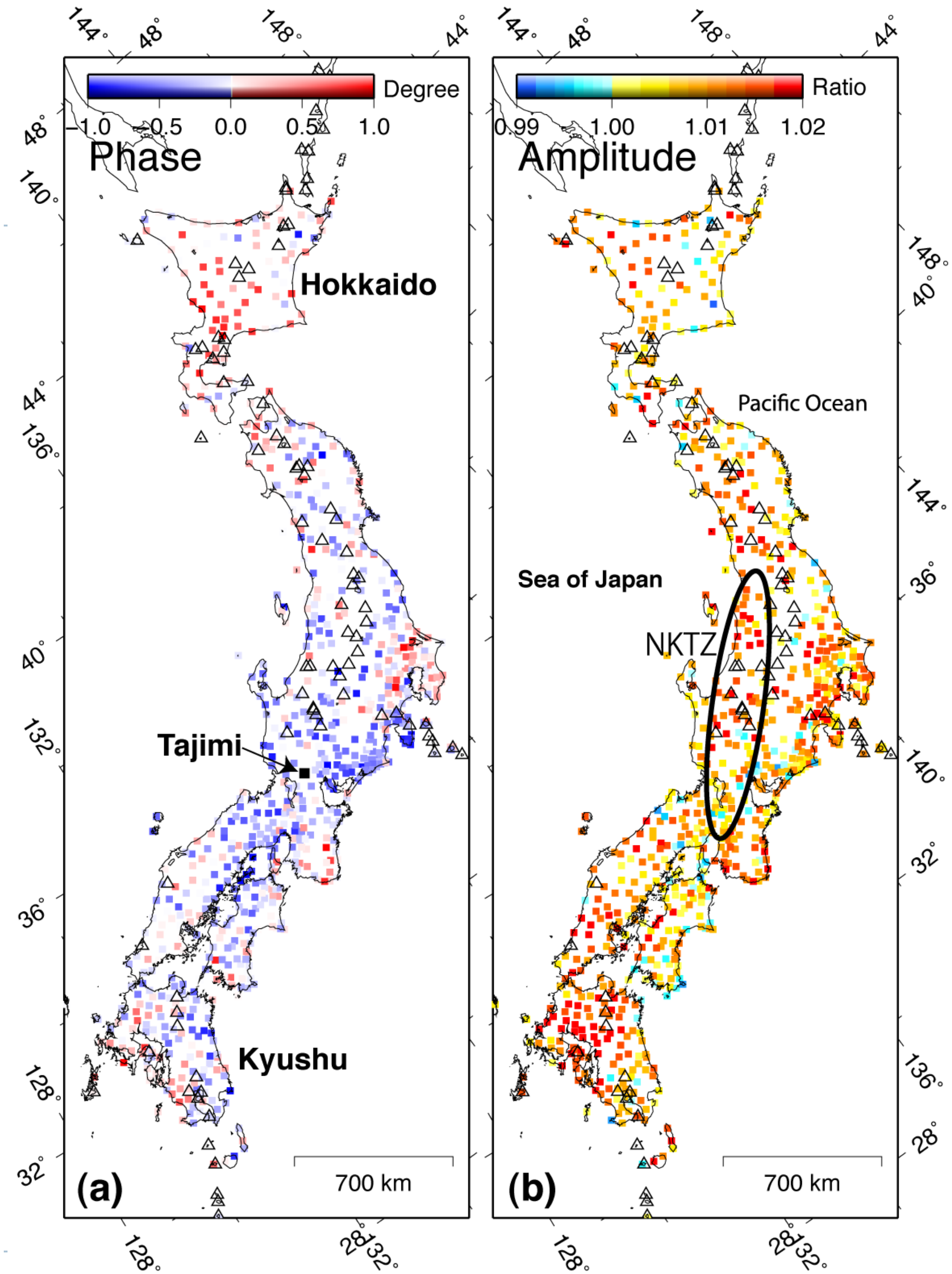

After Ito et al. (2009)

Conclusion (Part 1)

- We generated a high resolution map of the regional Earth tides response using KPPP GPS observations of the Japanese islands.
- Comparisons of the KPPP GPS results with SG observations confirmed the validity of the KPPP GPS analyses.
- The M2 tidal constituent derived from the vertical component of the displacement is the most robust and accurate observation.

Observation map

- 702 GPS observation (from PBO)
- Observation periods: 1/1/2008-12/31/2008
- Sampling rate: 5 minutes
- GPS software: Gps Tools [ver. 0.6.4]
- Ocean tidal load (OTL)

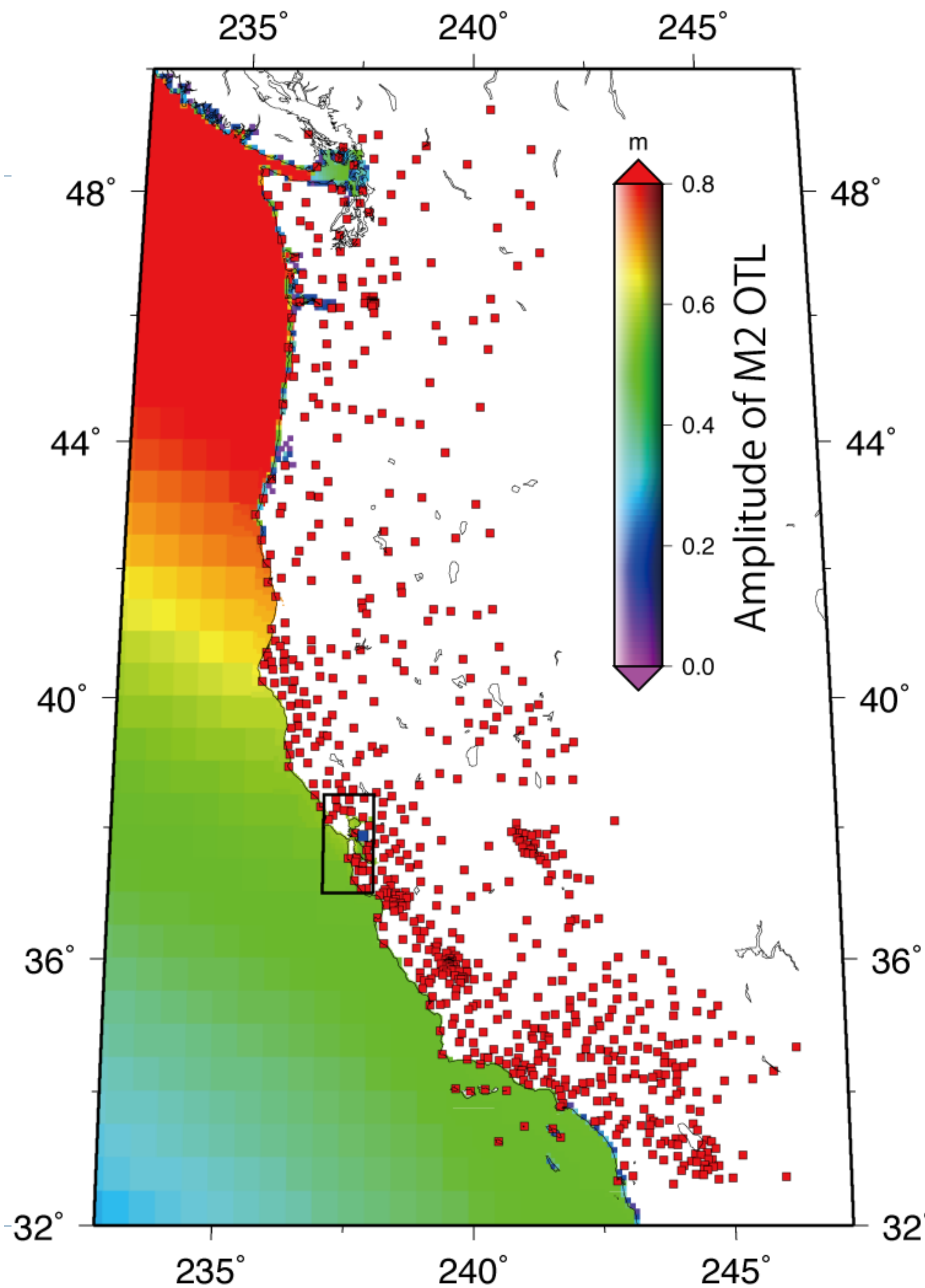

GPS observation [P224] (1/3)

- Observation = Body tide + OTL disp. + err
- Body tide is theoretical estimate.
  Use complex (attenuation) Love numbers with 500 tidal constituents and frequency dependence

Red: Predicted body tide
Black: GPS observation

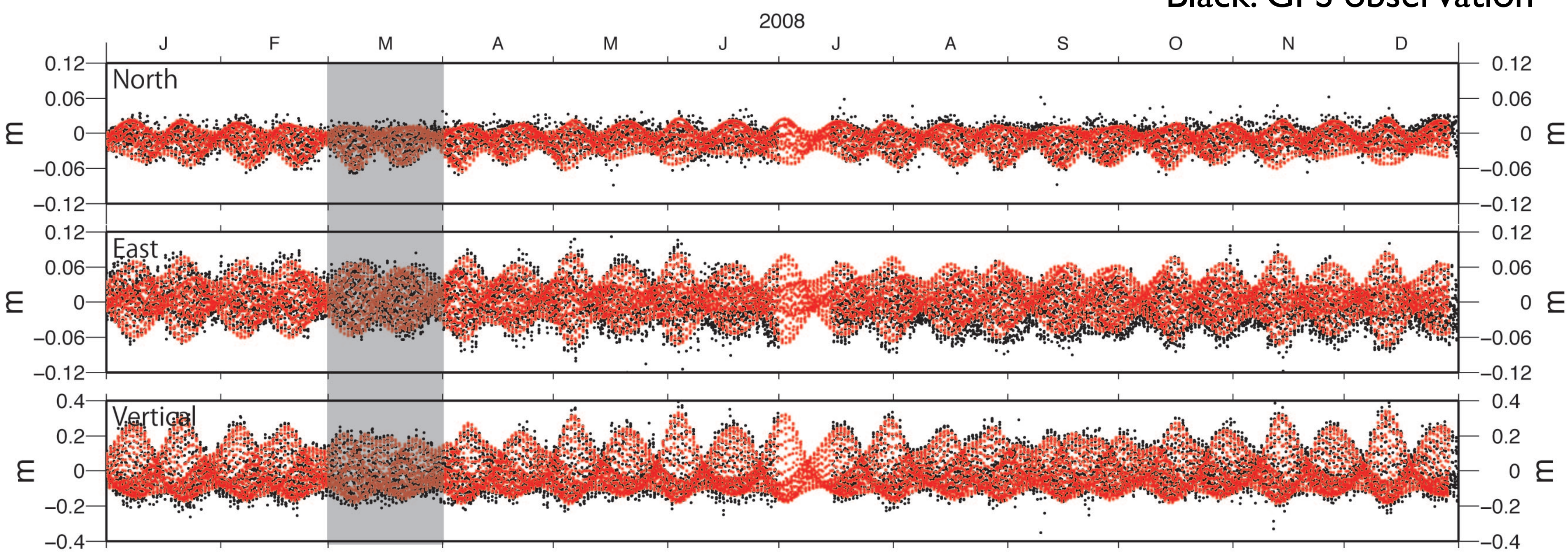

GPS observation [P224] (2/3)

- Observation = Body tide + OTL disp. + err
- Body tide is theoretical estimate.
  Use complex (attenuation) Love numbers with 500 tidal constituents and frequency dependence

Red: Predicted body tide
Black: GPS observation

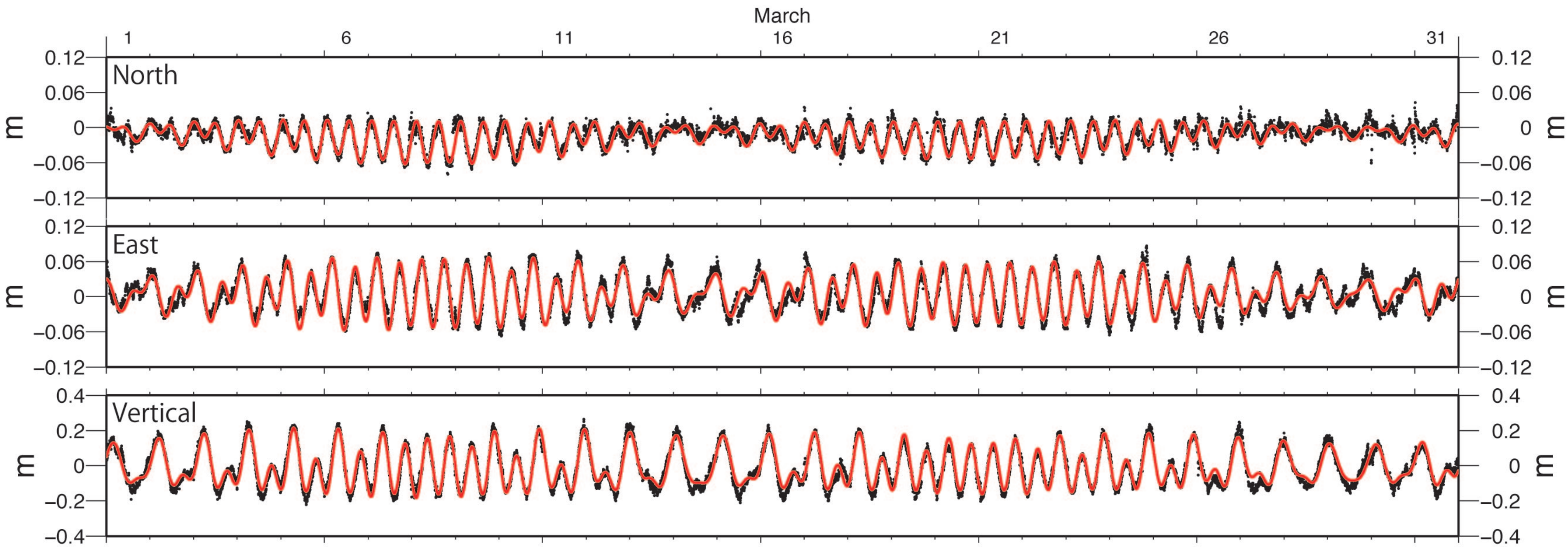

Body tide on a 3-D elastic earth

- Sensitivity of earth elastic structure to body tides is too small for detection by GPS.
- Although it may be possible to estimate the Earth inner structure.

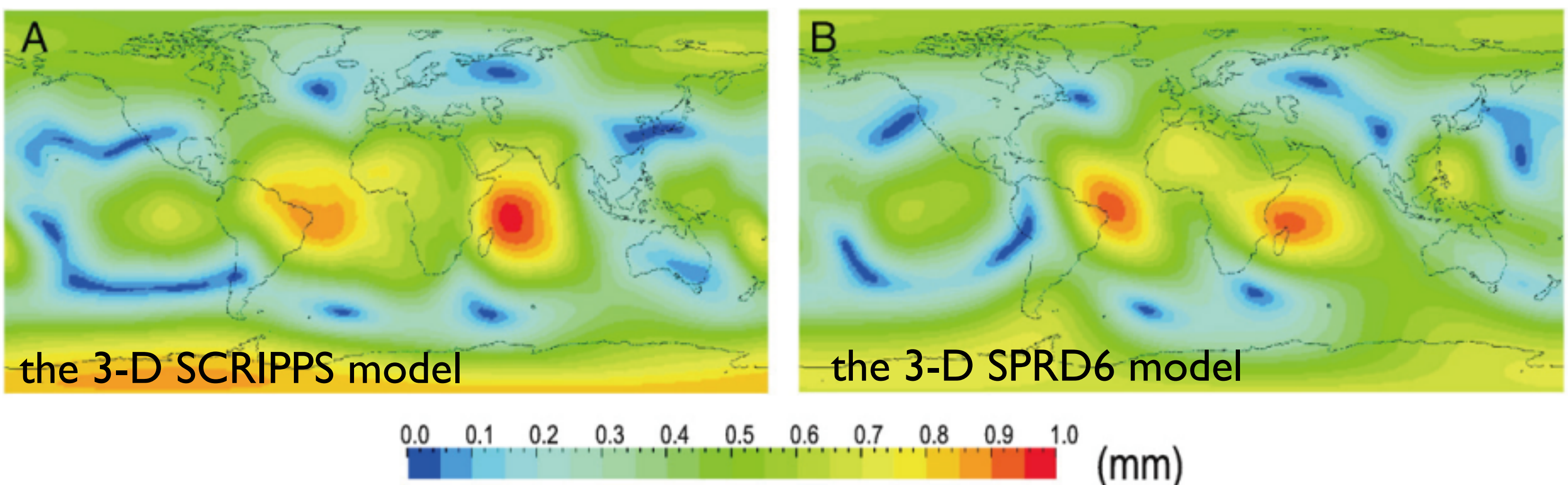

The maximum of the absolute value of the perturbation in the radial displacement body tide response computed using a 3-D models and PREM.

After Latychev et al. (2009)

GPS observation [P224] (3/3)

- Observation - Body tide = OTL disp. + err
- OTL disp. is estimated from observation.
- Applied Sidereal filter (remove multipath).

$$O(t) = \sum_{j=1}^{15}\{A_j^{OBS}\cos(\psi_j t) + B_j^{OBS}\sin(\psi_j t)\} + \sum_{n=3}^{\infty}\{C_n \cos(n\psi_{sidereal}t) + D_n \sin(n\psi_{sidereal}t)\} + \epsilon(t)$$

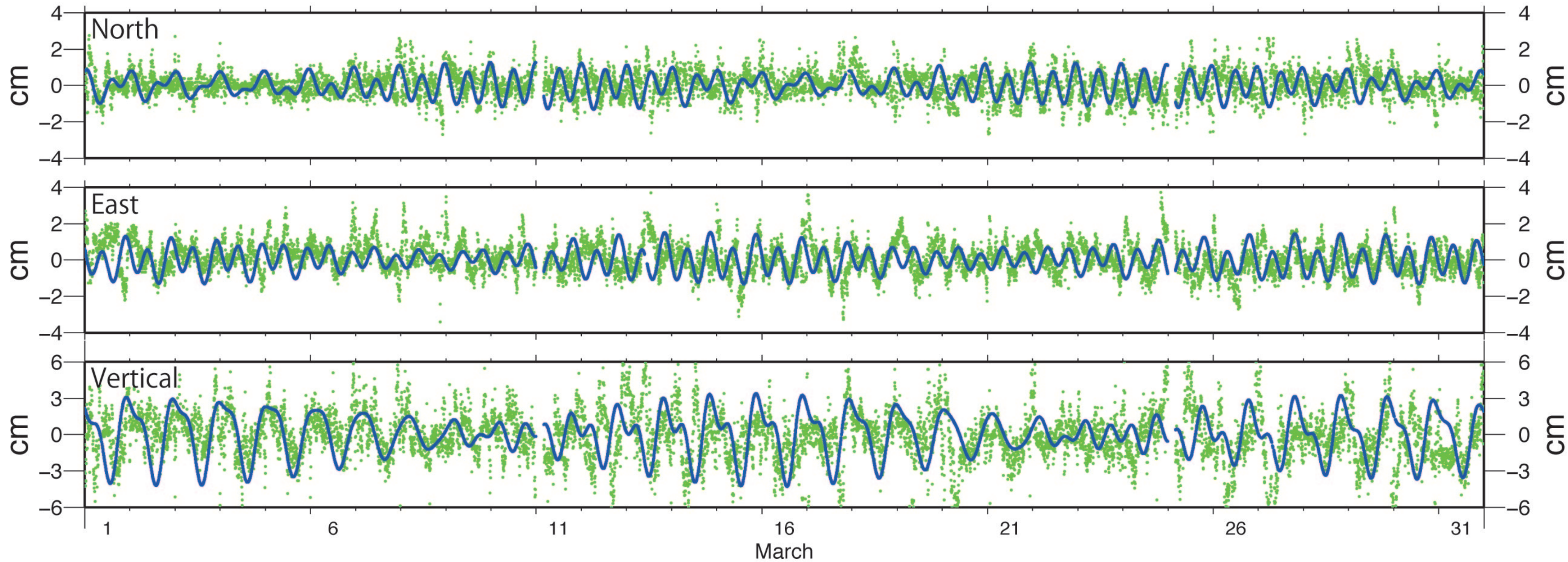

Green: GPS observation – Predicted Body tide
Blue: Estimated OTL response

Spatial distribution of the OTL response

- 3 components of M2 OTL

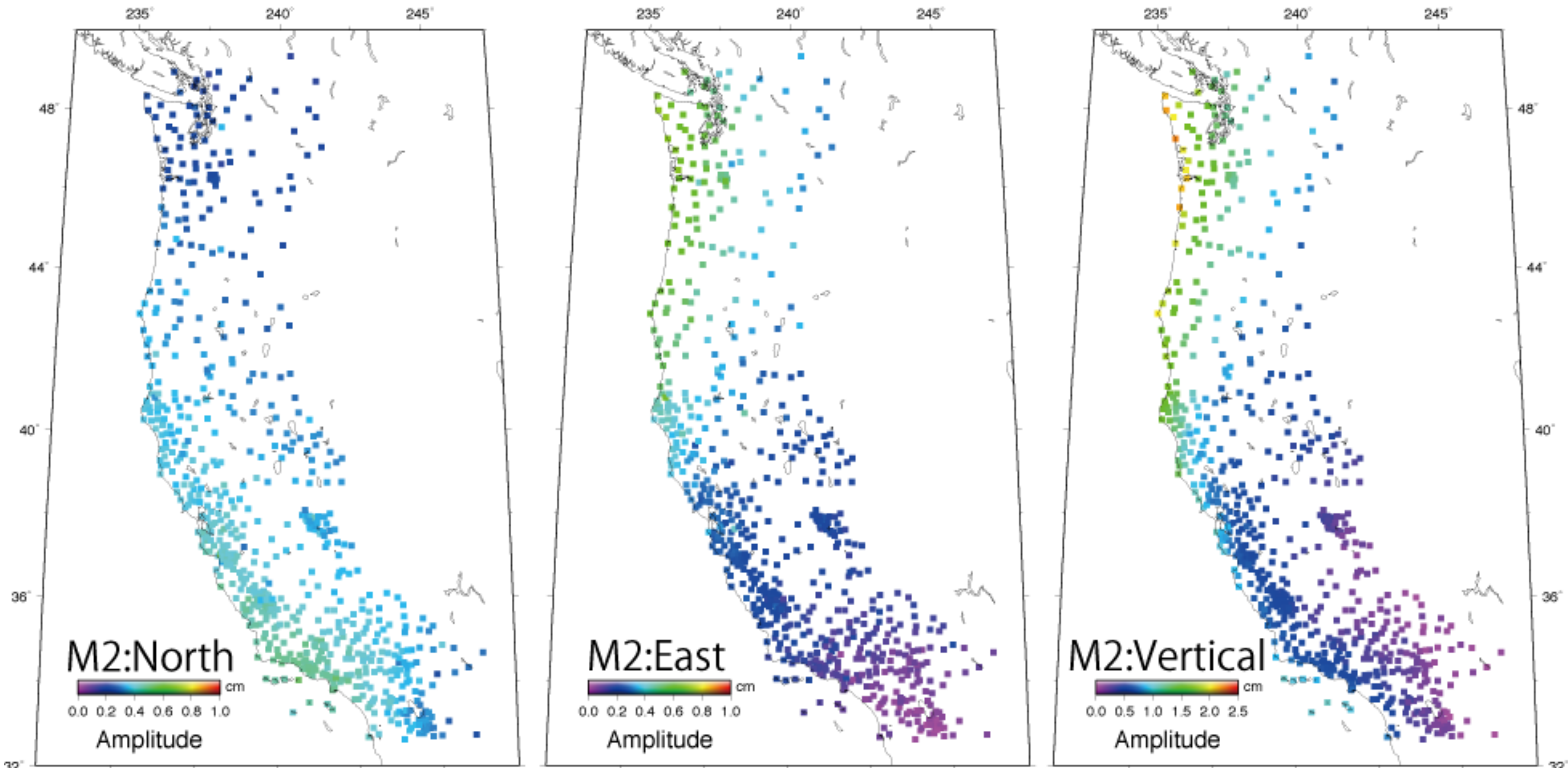

Observation error

- Estimated error [STD]

  North : 1.1 cm

  East : 1.3 cm

  Vertical : 2.7 cm

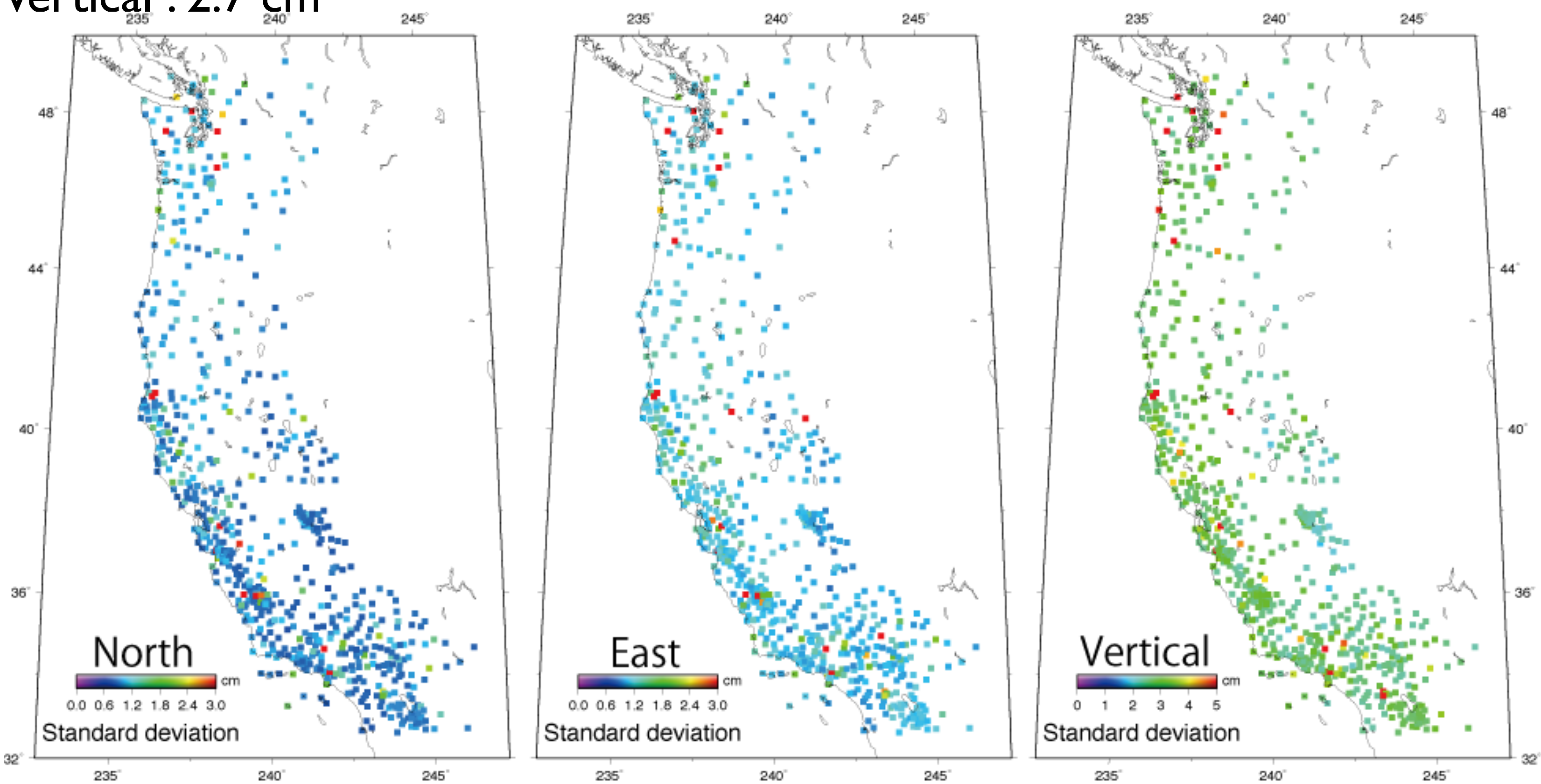

M2 North-South

Constituent: M2
Component: North-South
Variance Reduction:93.4%
Total Power: 2.52m

Model: FES2004+PREM

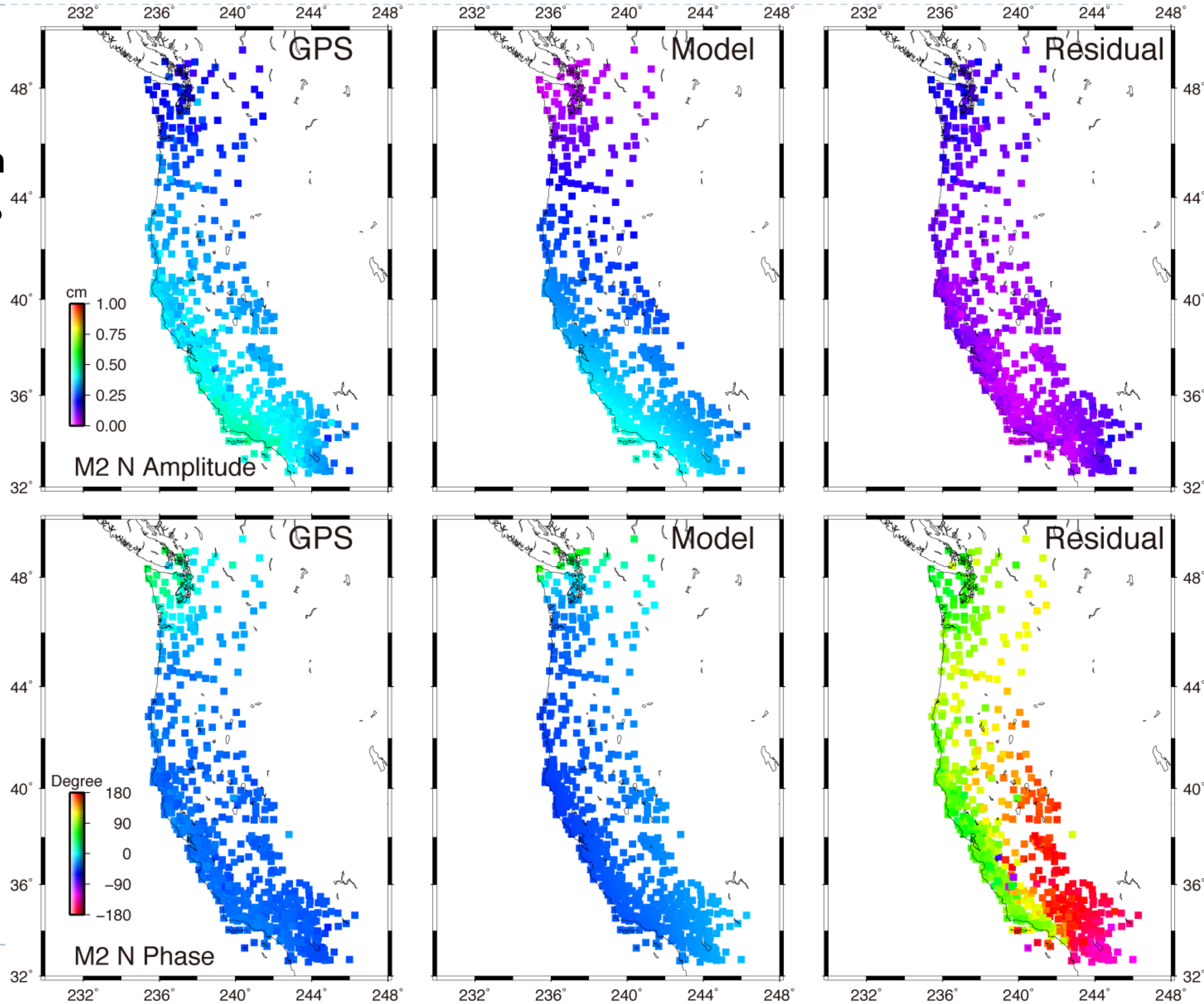

O1 Vertical

Constituent: O1
Component: Vertical
Variance Reduction: 93.4%
Total Power: 7.41m

Model: FES2004+PREM

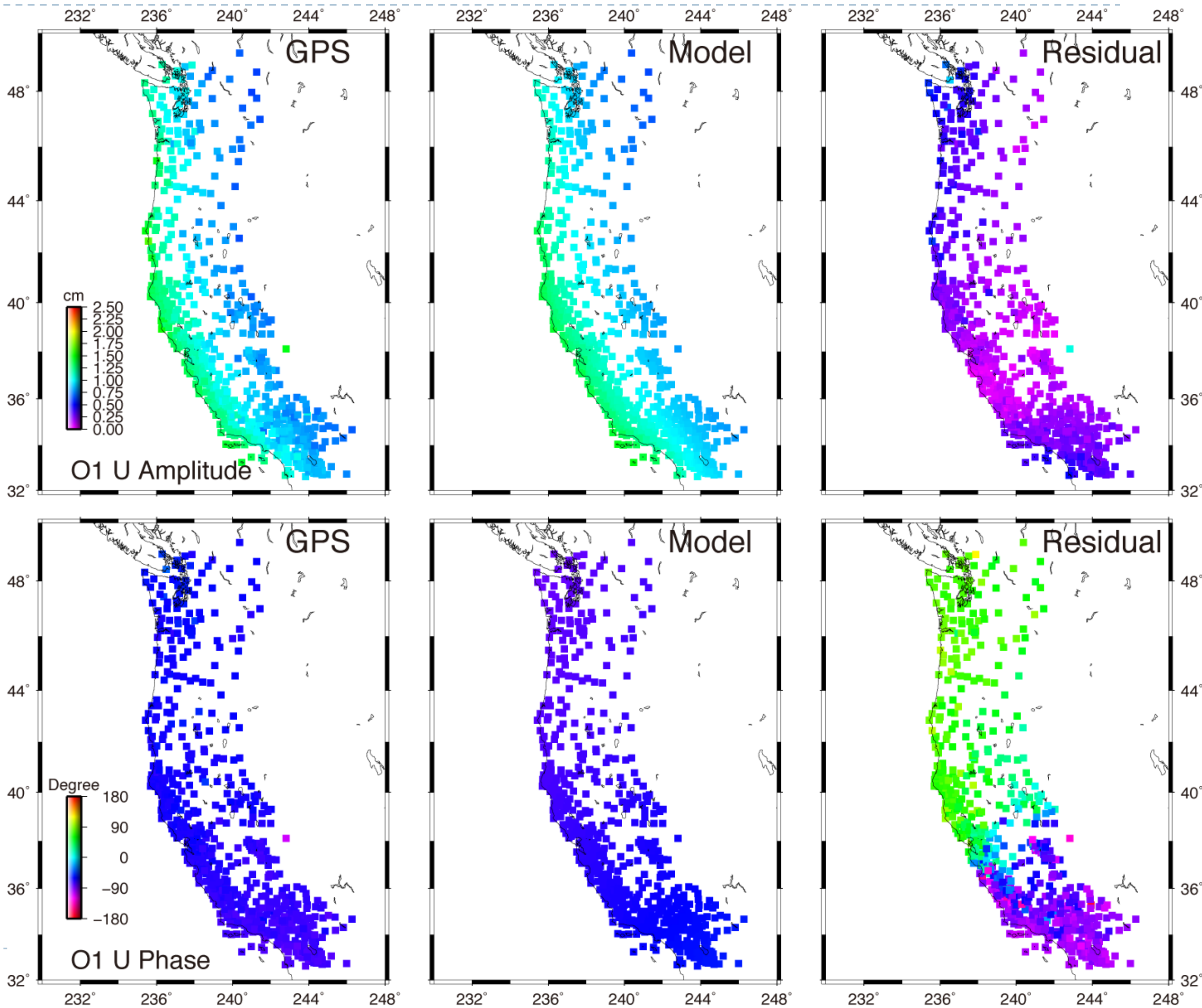

K1 East-West

Constituent: K1
Component: East-West
Variance Reduction:50.6%
Total Power: 3.10m

Model: FES2004+PREM

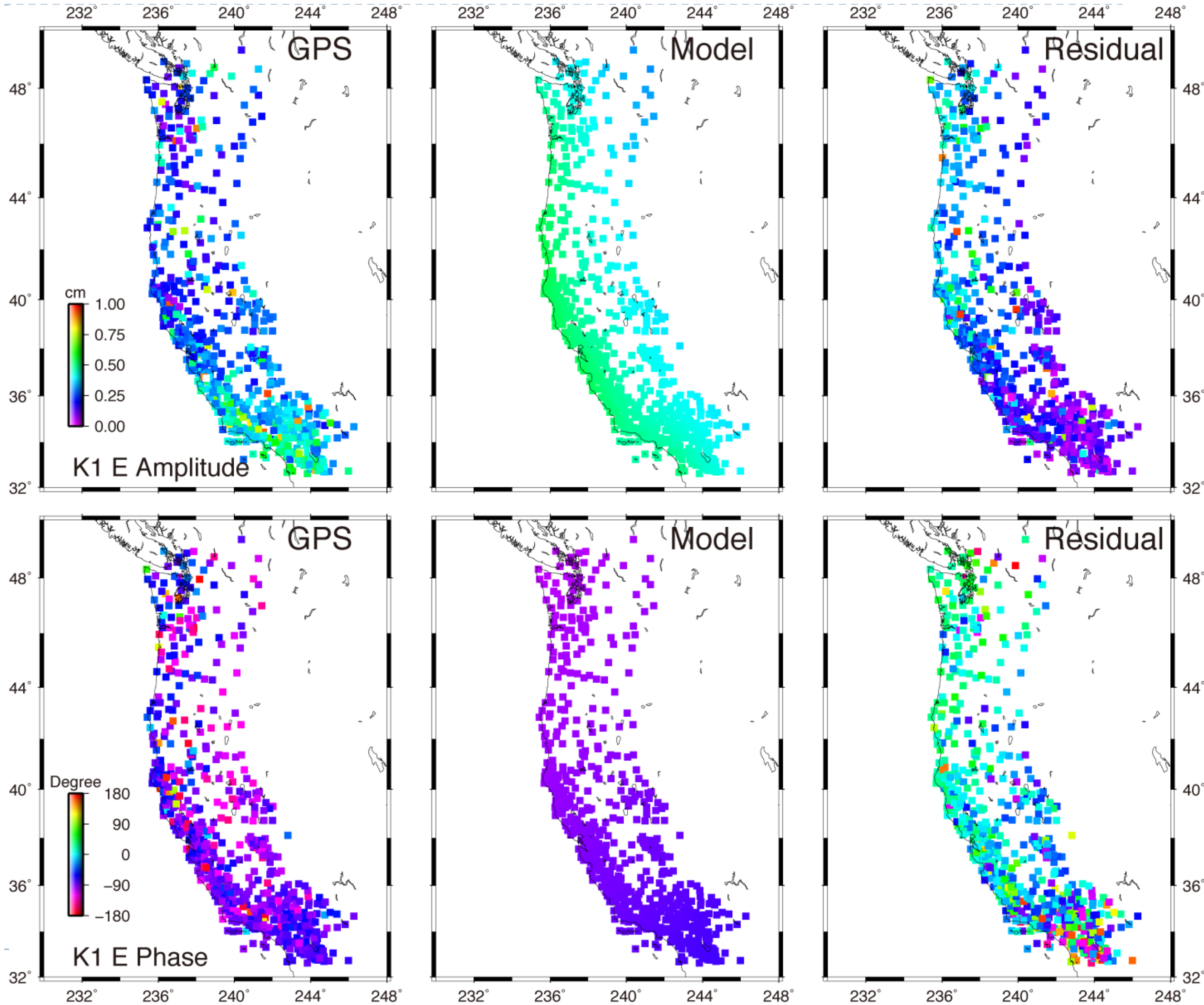

Variance reduction

		North		East		Vertical		Total	
Wave	Period	VR[%]	Amp.[m]	VR[%]	Amp.[m]	VR[%]	Amp.[m]	VR[%]	Amp.[m]
M2	12.42	93.4	(2.52)	74.7	(1.30)	61.6	(3.72)	74.5	(7.54)
K1	23.93	61.0	(1.62)	50.6	(3.10)	83.1	(11.67)	74.8	(16.39)
S2	12.00	76.8	(1.09)	38.6	(0.56)	59.7	(2.49)	61.3	(4.14)
O1	25.82	73.4	(1.03)	89.8	(2.01)	93.4	(7.41)	90.7	(10.45)
P1	24.07	48.9	(0.53)	60.9	(1.02)	74.0	(3.85)	69.1	(5.40)
N2	12.66	81.2	(0.57)	43.9	(0.22)	44.5	(0.62)	59.2	(1.41)
K2	11.97	0.3	(0.02)	0.3	(0.02)	2.3	(0.15)	1.9	(0.19)
Mf	327.86	18.3	(0.05)	31.3	(0.11)	32.4	(0.21)	30.1	(0.37)
Q1	26.87	57.1	(0.20)	67.3	(0.37)	76.1	(1.35)	72.4	(1.92)
Mm	661.31	7.2	(0.02)	9.9	(0.04)	13.5	(0.10)	11.8	(0.16)
2N2	12.91	43.3	(0.08)	11.7	(0.03)	21.9	(0.13)	27.8	(0.24)
Mtm	219.19	3.7	(0.01)	8.0	(0.03)	9.0	(0.05)	8.1	(0.09)
S1	24.00	4.7	(0.04)	4.1	(0.06)	6.2	(0.16)	5.5	(0.26)
M4	6.21	2.2	(<0.01)	1.6	(<0.01)	3.5	(<0.01)	2.4	(<0.01)
Msqm	170.30	0.6	(<0.01)	1.1	(<0.01)	1.2	(<0.01)	1.0	(<0.01)

Using OTL to estimate elastic structure: Inversion method(1/2)

- Non-linear observation equation

$$\mathbf{d} = g(\mathbf{m})$$

- Unknown parameters are
  elastic moduli and density vs. depth.

$$\mathbf{m} = \{\log \frac{\lambda}{\lambda_0}, \log \frac{\mu}{\mu_0}, \log \frac{\rho}{\rho_0}\}$$

- Inverse linearized approach based on Levenberg-Marquardt algorithm

  Total unknown parameters: 249

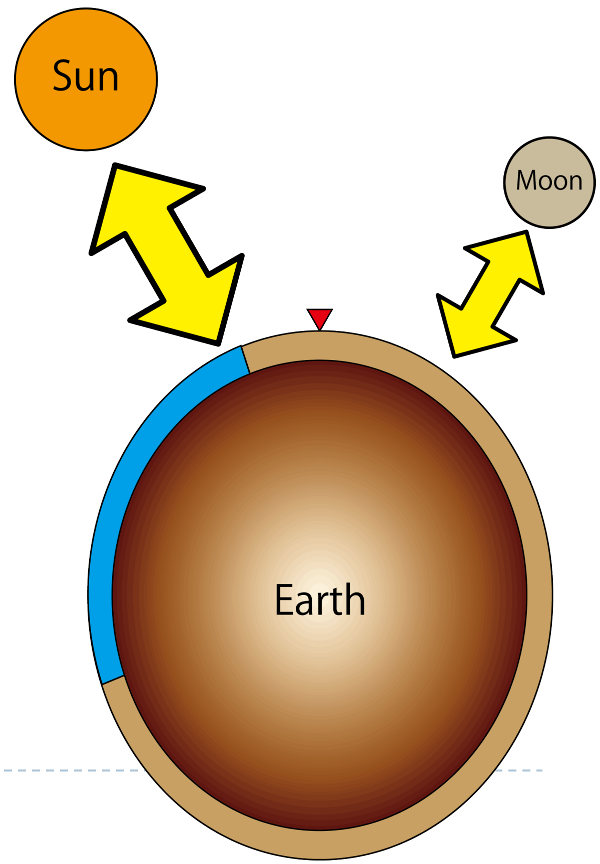

Inversion method(2/2)

- Constrain
  Total mass of the Earth
  dynamical moment of inertia of the Earth [I/MR^2]
- Smoothing hyper-parameter

$$ABIC(\sigma^2, \alpha^2) = -2\log[p(\mathbf{d}|\sigma^2, \alpha^2)] + 2N_p$$

$$\begin{aligned} p(\mathbf{d}|\sigma^2, \alpha^2) &= \int_{-\infty}^{+\infty} p(\mathbf{d}|\mathbf{m}^*, \sigma^2) p(\mathbf{m}^*|\alpha^2) d\mathbf{m}^* \\ &= (2\pi\sigma^2)^{-\frac{N}{2}} (\alpha^2)^{-\frac{M}{2}} |\Sigma_d|^{-\frac{1}{2}} |\mathbf{C}^T\mathbf{C}|^{\frac{1}{2}} \\ &\quad |\frac{1}{\sigma^2} g(\mathbf{m}^*)^T \Sigma_d^{-1} g(\mathbf{m}^*) + \frac{1}{\alpha^2} \mathbf{C}^T\mathbf{C}|^{-\frac{1}{2}} \exp[-\frac{1}{2}\Psi(\mathbf{m}^*)] \end{aligned}$$

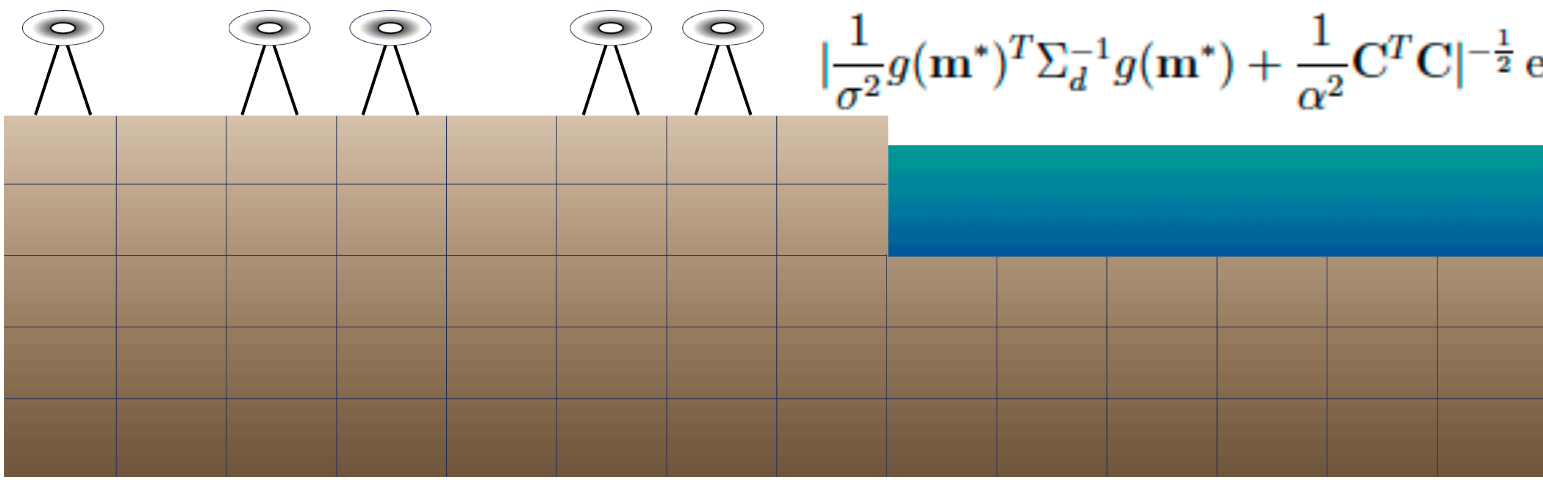

Fine mesh

- 3 different resolutions
  1st order grid [0.5° by 0.5°]
  2nd order grid [5’by 5’]
  3rd order grid [1’ by 1’]

  3rd ＜[5°] ≦2nd ＜[30°]≦1st

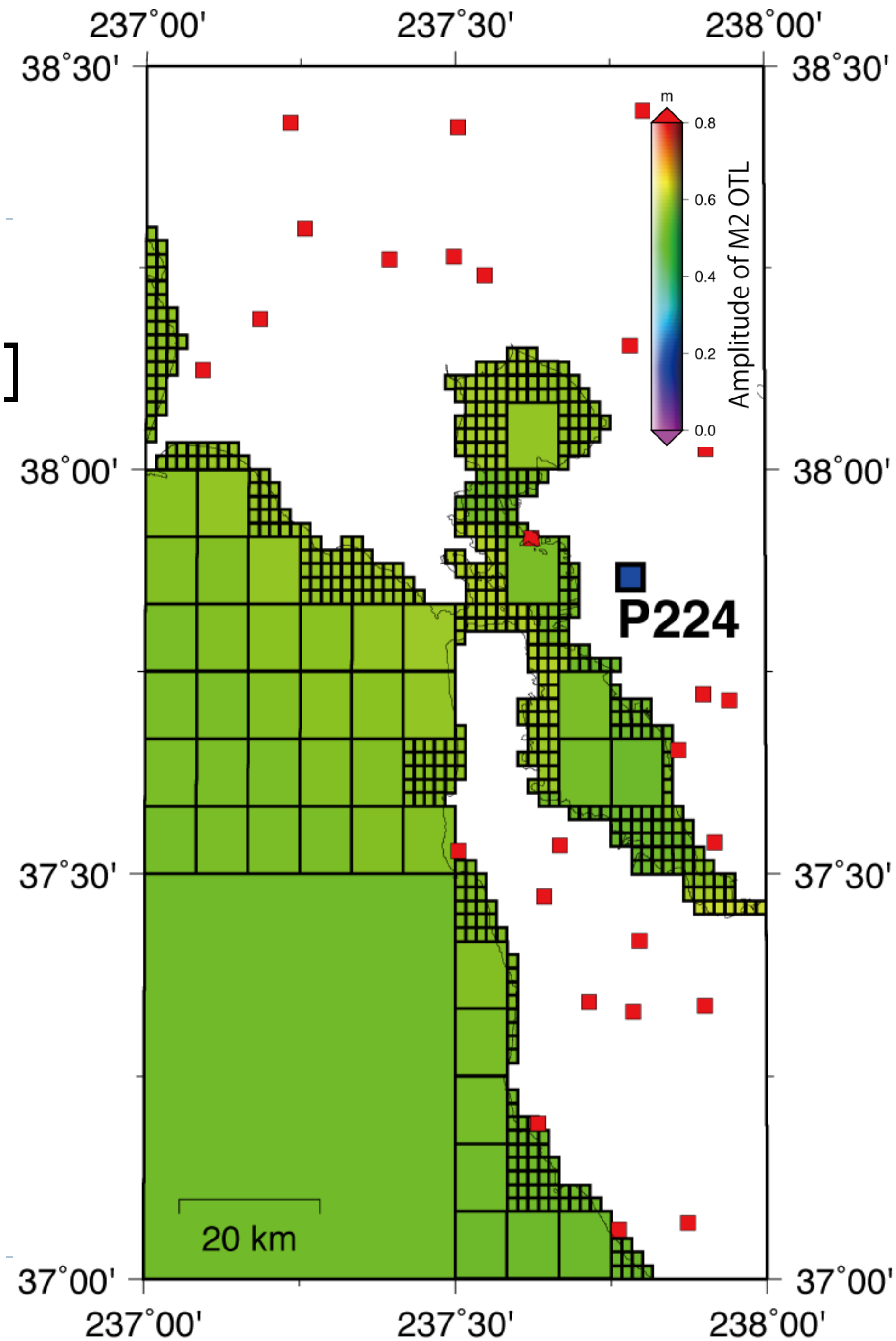

Load Green function

- Q effects

$$\begin{cases} \mu(T) = \mu(1)\left(1 - \frac{\ln T}{\pi}\frac{1}{Q_\mu}\right) \\ \lambda(T) = \lambda(1)\left[1 - \frac{\ln T}{\pi}\left(\frac{1+\gamma}{Q_\kappa} - \frac{\gamma}{Q_\mu}\right)\right] \end{cases}$$

where $\gamma = \frac{2}{3}(\frac{\mu}{\lambda})$

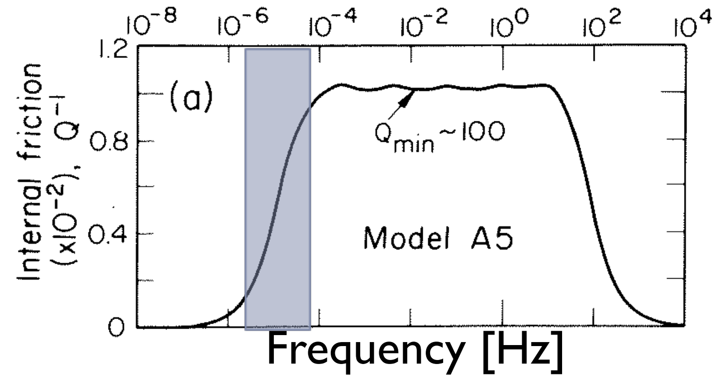

- SNREI Earth model

  the spherically symmetrical, non-rotating, perfectly elastic and isotropic Earth model

Sensitivity Kernel of Load Green function

$$K(R, \mathbf{S}) = \frac{G(R, \mathbf{S} + \delta\mathbf{S})}{G(R, \mathbf{S})}$$

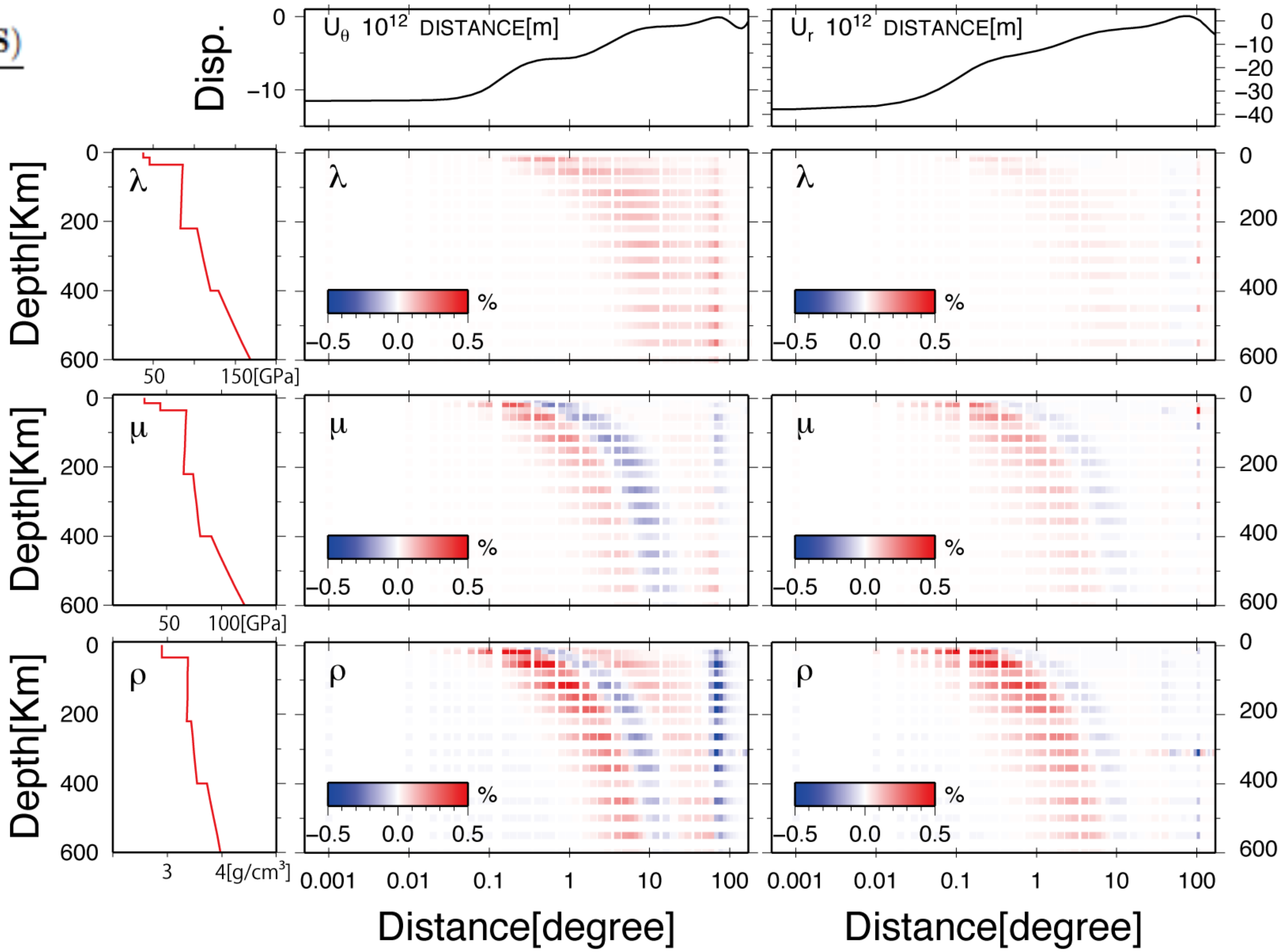

Compare global ocean tides models

	NAO.99b	GOT99.2b	CSR4.0	Schwiderski	FES2004
VR	74.01	74.19	74.23	68.79	75.48

NAO.99b [assimilation model]: *Matsumoto et al. [2000]*
GOT99.2b [empirical model]: *Ray [1999]*
CSR4.0 [empirical model]: *Eanes and Bettadpur [1994]*
Schwiderski [a purely hydrodynamical model] : *Schwiderski [1980]*
FES2004 [assimilation model]: *Lyard et al. [2006]*.

1-D model

- Our 1-D model
  VR:77.13%
- PREM
  VR:75.43%

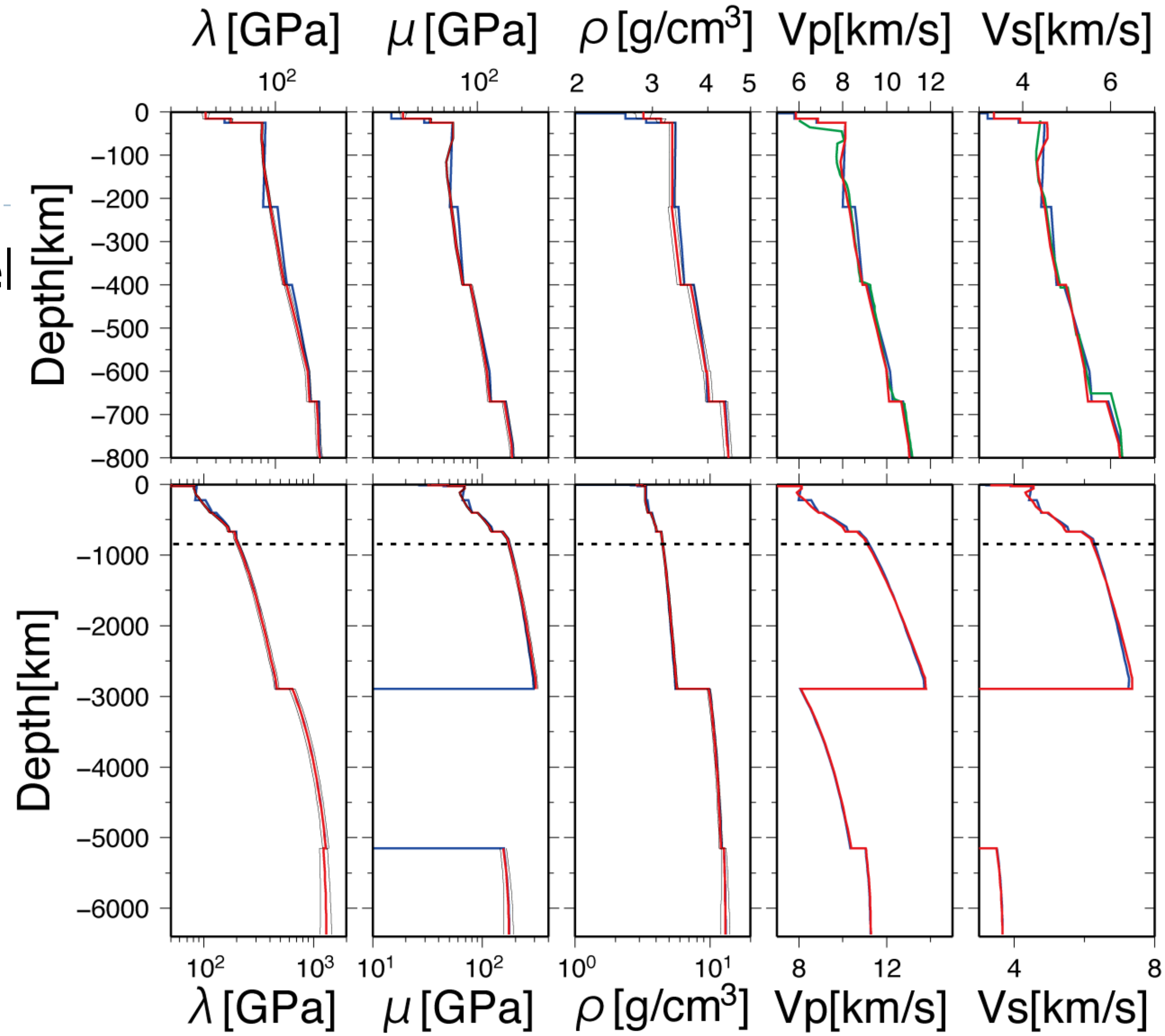

Red: our 1-D model
Blue: PREM
Green of VP: T7 (Burdick and Helmberger [1978])
Green of VS: TNA (Grand and Helmberger [1984]).

1-D model

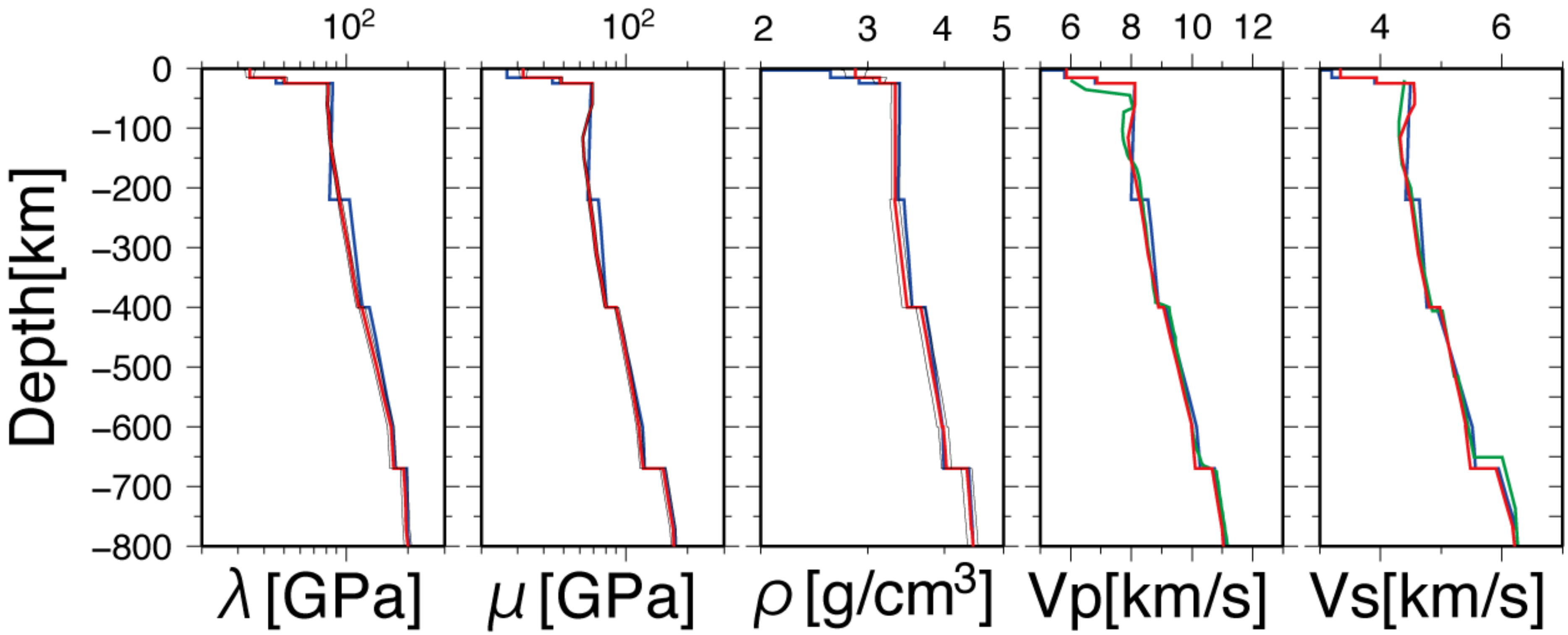

Our 1-D model
VR:77.13%
PREM
VR:75.43%

Red: our 1-D model
Blue: PREM
Green of VP: T7 (Burdick and Helmberger [1978])
Green of VS: TNA (Grand and Helmberger [1984]).

Histogram of residual (1/2)

- PREM
  Mean: 0.66 mm
  STD:1.60 mm

- Our 1-D model
  Mean: 0.42 mm
  STD: 1.53 mm

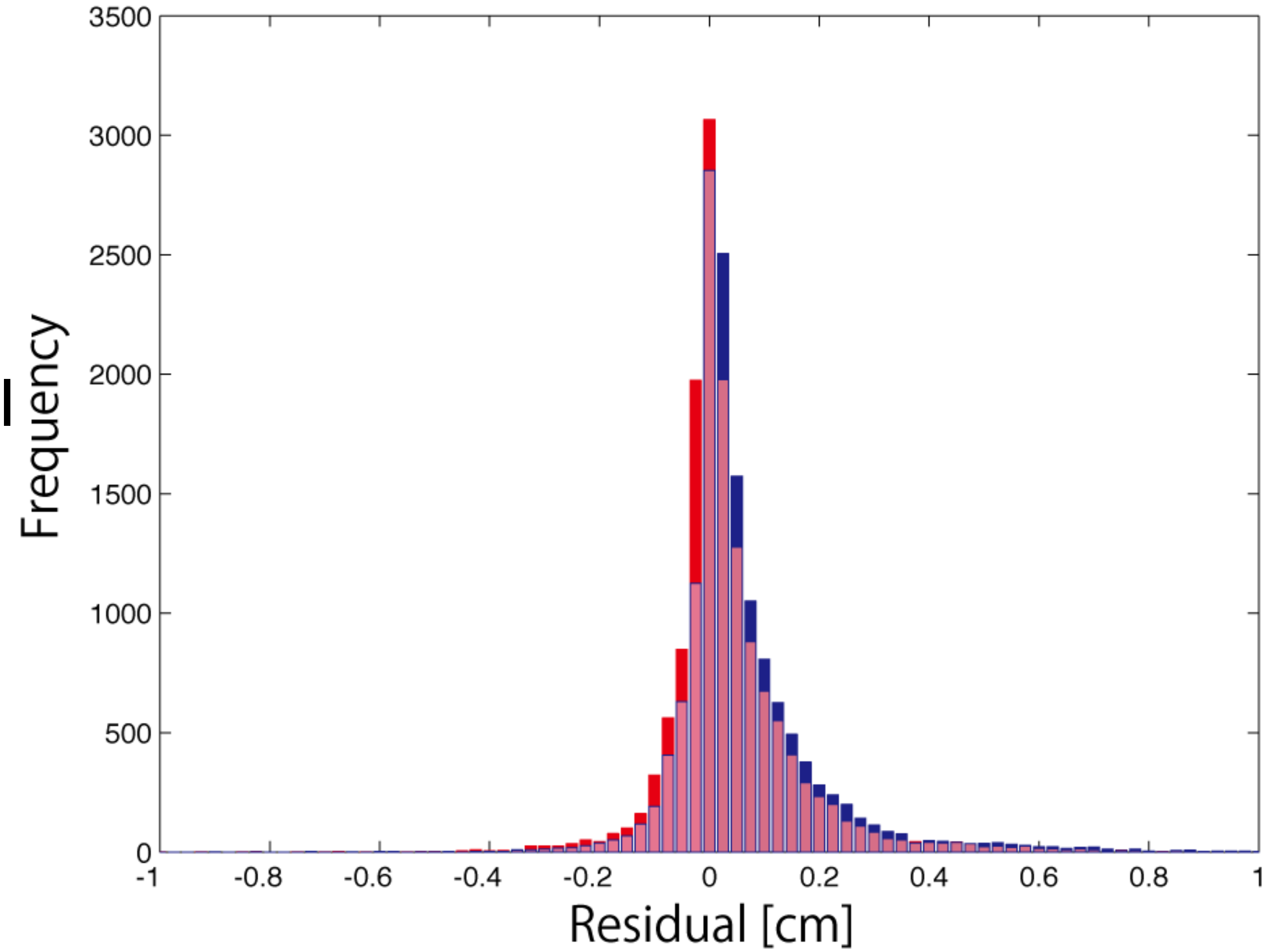

Red: our 1-D model
Blue: PREM

Histogram of residual (2/2)

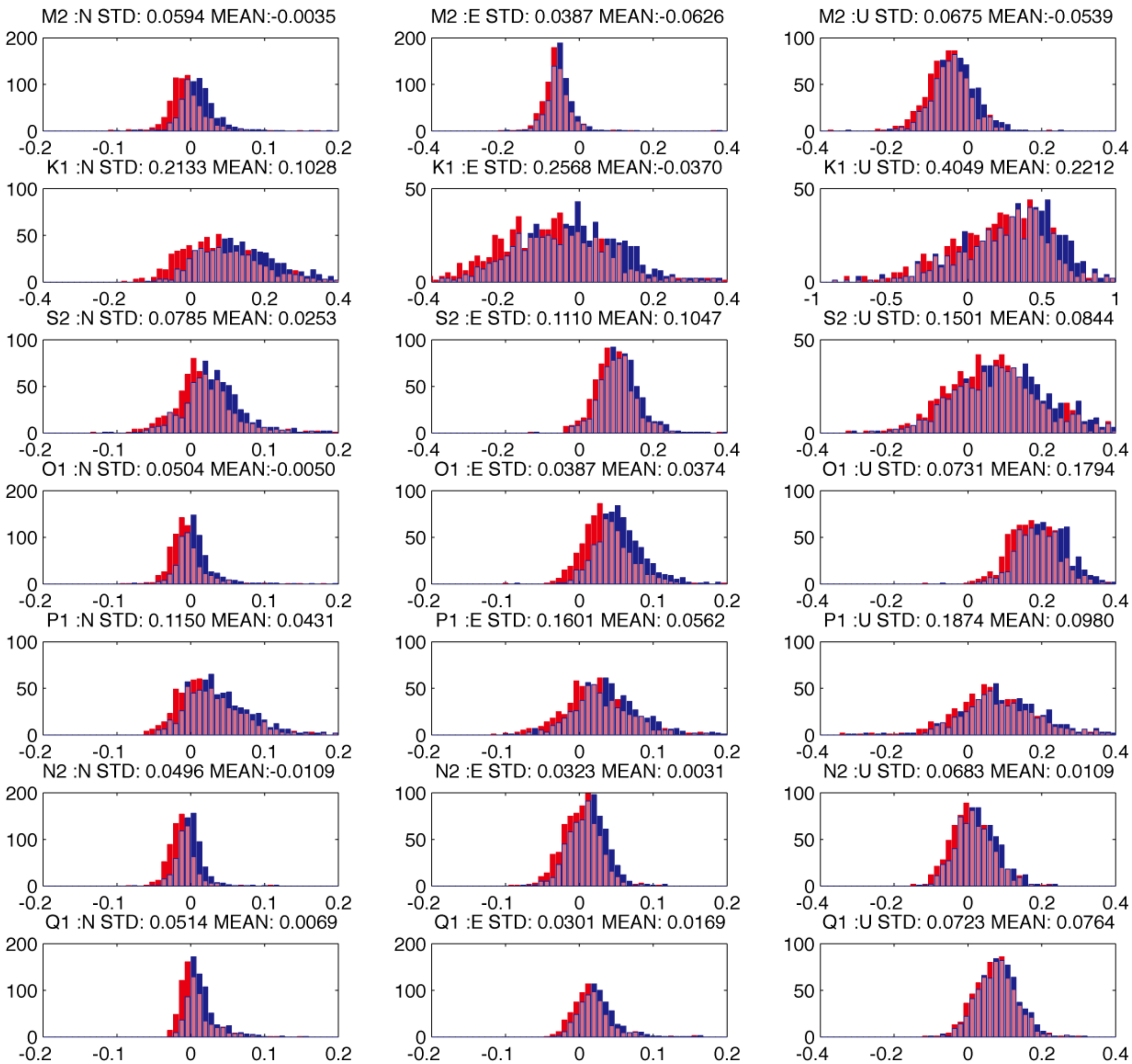

Unit:cm

Spatial distribution of residual (1/2)

- Residual from final estimated 1D model
- Spatial coherency suggests need for 3D model in the future.

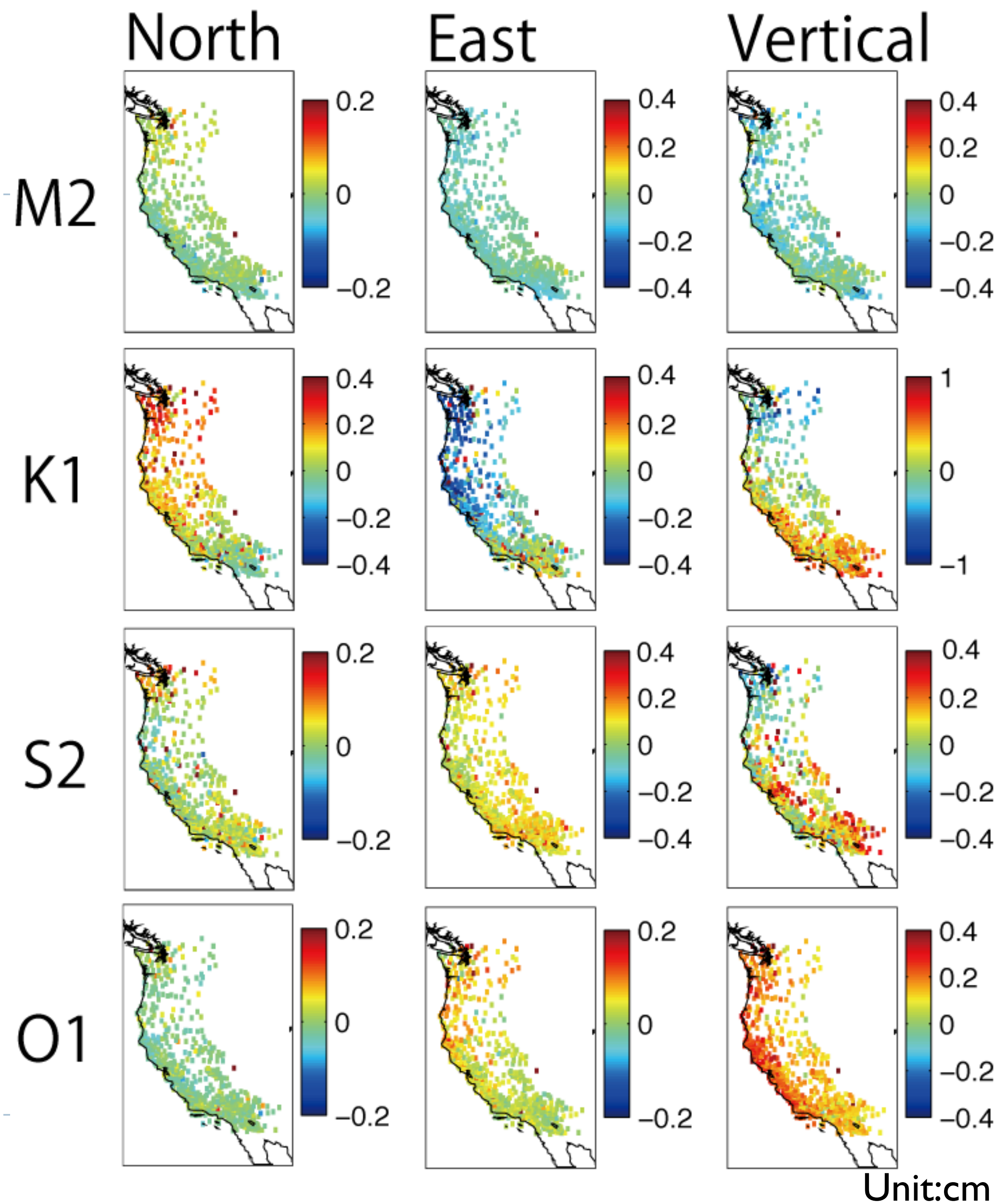

Spatial distribution of residual (2/2)

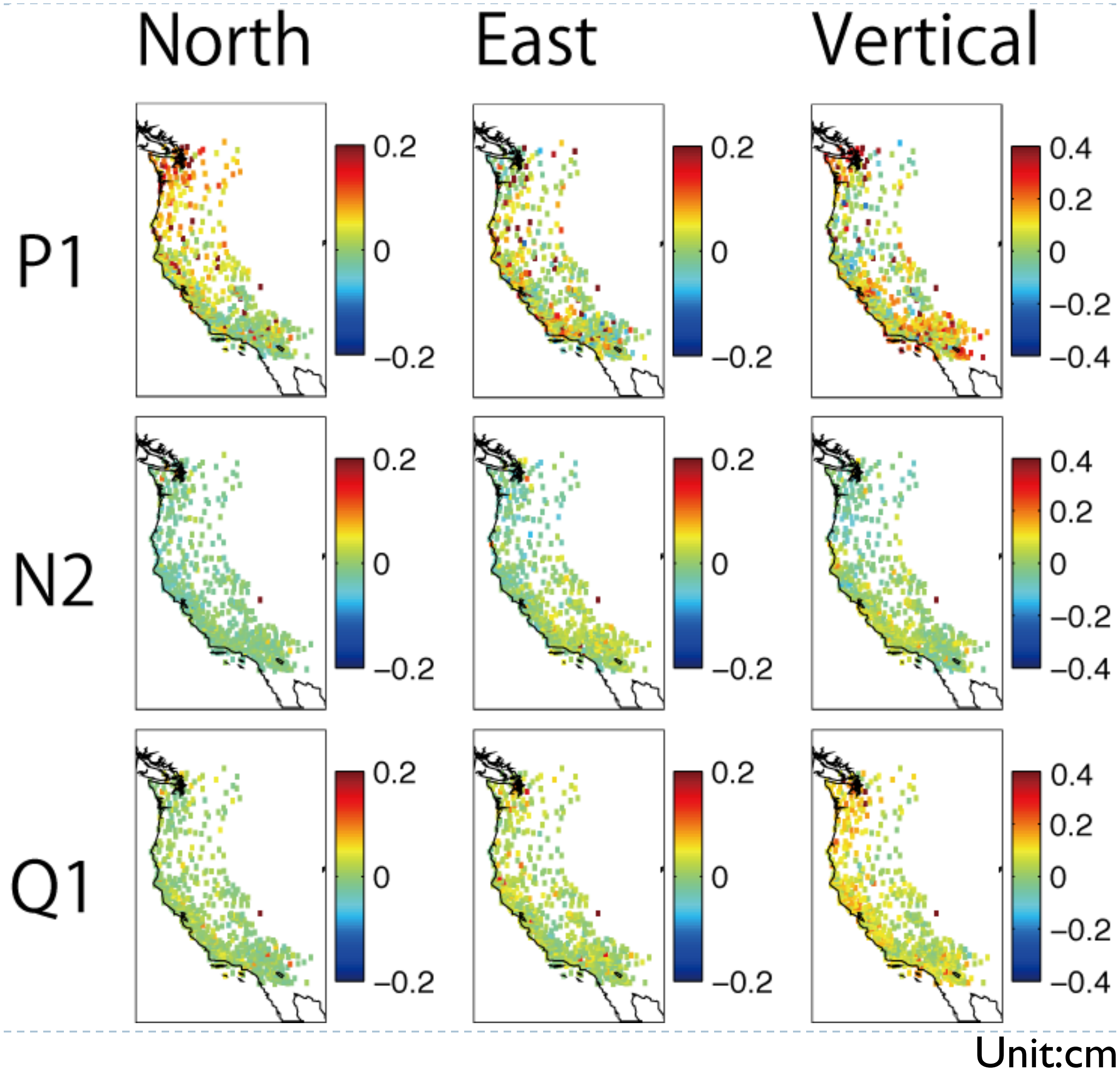

Known Issues:

- Use of mass and moment of inertia constraint may not be appropriate for a regional study.
- Currently using a gradient search technique, and we are concerned about local minima and correlations between moduli and density
- Coherent spatial residual suggest a need for 3D variations

Conclusion (Part 2)

- We generate a large collection of OTL response data (M2, K1, S2, O1, P1, N2 and Q1) from GPS data.
- We have demonstrated that OTL response data from GPS can constrain independent regional variation in λ, μ, and ρ.
- Our 1-D model are consistent with existing global travel-time models.
- The main differences are in the upper mantle where we infer a low-velocity zone from our 1-D model.